

# Quantification of Proteins Involved in Drug Metabolism and Disposition in the Human Liver Using Label-Free Global Proteomics

Narciso Couto,<sup>\*,§,†,⊥</sup> Zubida M. Al-Majdoub,<sup>§,⊥</sup> Brahim Achour,<sup>§</sup> Phillip C. Wright,<sup>†,||</sup> Amin Rostami-Hodjegan,<sup>§,‡</sup> and Jill Barber<sup>\*,§</sup>

<sup>§</sup>Centre for Applied Pharmacokinetic Research, University of Manchester, Stopford Building, Oxford Road, Manchester M13 9PT, U.K.

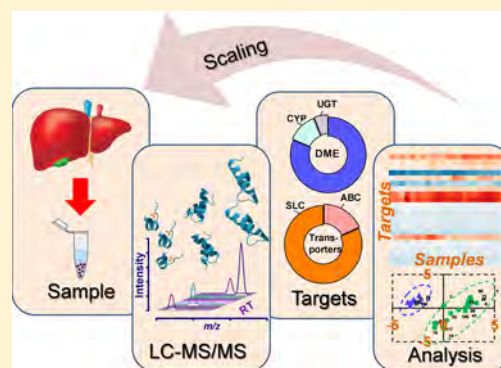
<sup>†</sup>Department of Chemical and Biological Engineering, ChELSI Institute (Chemical Engineering at the Life Science Interface), University of Sheffield, Sir Robert Hadfield Building, Mappin Street, Sheffield S1 3JD, U.K.

<sup>‡</sup>Simcyp Ltd. (a Certara company), 1 Concourse Way, Sheffield S1 2BJ, U.K.

## Supporting Information

**ABSTRACT:** There is an urgent need (recognized in FDA guidance, 2018) to optimize the dose of medicines given to patients for maximal drug efficacy and limited toxicity (precision dosing), which can be facilitated by quantitative systems pharmacology (QSP) models. Accurate quantification of proteins involved in drug clearance is essential to build and improve QSP models for any target population. Here we describe application of label-free proteomics in microsomes from 23 human livers to simultaneously quantify 188 enzymes and 66 transporters involved in xenobiotic disposition, including 17 cytochrome P450s (CYPs), 10 UDP-glucuronosyltransferases (UGTs), 7 ATP-binding cassette (ABC) transporters, and 11 solute carrier (SLC) transporters; six of these proteins are quantified for the first time. The methodology allowed quantification of thousands of proteins, allowing estimation of sample purity and understanding of global patterns of protein expression. There was overall good agreement with targeted quantification and enzyme activity data, where this was available. The effects of sex, age, genotype, and BMI on enzyme and transporter expression were assessed. Decreased expression of enzymes and transporters with increasing BMI was observed, but a tendency for older donors to have higher BMIs may have confounded this result. The effect of genotype on enzymes expression was, however, clear-cut, with CYP3A5\*1/\*3 genotype expressed 16-fold higher compared with its mostly inactive \*3/\*3 counterpart. Despite the complex, time-consuming data analysis required for label-free methodology, the advantages of the label-free method make it a valuable approach to populate a broad range of system parameters simultaneously for target patients within pharmacology and toxicology models.

**KEYWORDS:** human liver microsomes, cytochrome P450, uridine 5'-diphosphate-glucuronosyltransferase, ATP-binding cassette transporters, solute carrier transporters, label-free proteomics



## INTRODUCTION

Quantitative systems pharmacology (QSP) models, such as physiologically based pharmacokinetic (PBPK) models, are increasingly used to predict appropriate doses of drugs for patient groups, especially groups that may not be assessed during clinical trials (young, old, pregnant, and chronically diseased patients, for example). Over 30 recent drug labels have benefitted from model-informed decisions about dosing in lieu of clinical studies.<sup>1,2</sup> Publication of the final FDA guidance on using PBPK models is another indication of the fact that these models are here to stay.<sup>3</sup>

In the human liver, cytochrome P450 (CYP) and uridine 5'-diphosphate-glucuronosyltransferase (UGT) enzymes, in combination with uptake and efflux transporters, play a vital role in the disposition of most drugs and xenobiotics. Because of factors such as genetic predisposition, lifestyle choices, age,

and disease, the expression of these proteins varies considerably among individuals.<sup>4</sup> As a result, drug treatments can vary in efficacy from patient to patient and toxic side effects may develop in certain populations.<sup>4</sup> The reliable prediction of drug behavior and safety across all populations is of paramount importance to the design and development of novel drugs and is of considerable value to pharmaceutical industries and regulatory authorities.<sup>1,5</sup>

The abundance of specific proteins in the human liver has been measured in either tissue lysates or enriched microsomal fractions, using targeted mass spectrometry-based quantitative

**Received:** September 6, 2018

**Revised:** November 24, 2018

**Accepted:** January 3, 2019

**Published:** January 4, 2019

proteomics approaches, which require the use of stable isotope-labeled standards, either in the form of concatenated proteotypic peptides (QconCAT) or as synthetic peptides (AQUA).<sup>6–11</sup> The crucial requirement of such targeted proteomic approaches is a set of unique peptides per protein under study with proven flyability in the mass spectrometer.<sup>12</sup> The use of targeted proteomics approaches for the quantification of CYPs, UGTs, and transporters has resulted in disparities in reported protein abundances.<sup>13</sup> This can be attributed to interlaboratory variability in the choice of standard peptides. In addition, differences in sample preparation methods and the technical difficulties presented by these proteins, particularly the high level of sequence similarity between the proteins within their respective subfamilies, have obscured genuine interindividual differences in protein expression.<sup>13</sup> The lack of a standardized, systematic methodology for all steps in the quantification of protein abundance, from tissue collection to mass spectrometric analysis, has recently been recognized as a major obstacle to generating consistent proteomic data.<sup>14,15</sup> A further inherent limitation of targeted proteomics is that the number of proteins that can be simultaneously analyzed is limited. Therefore, a comprehensive investigation of all relevant drug metabolizing enzymes and transporters using targeted proteomics is time-consuming and costly. The resource implications of targeted versus untargeted analysis have been previously analyzed and shown that the targeted methodology is not economically justified when a comprehensive analysis of drug metabolizing enzymes and transporters is desired.<sup>16</sup> Label-free proteomic quantification of drug metabolizing enzymes and transporters is therefore an attractive alternative. Label-free methods do not require the prior manual selection of unique peptides for protein quantification; instead, protein quantification is based on the intensities of peaks corresponding to all unique peptides detected by the mass spectrometer.<sup>17,18</sup> The advantage of label-free methods is that they enable the simultaneous quantification of large numbers of proteins allowing a systems-level understanding of the protein complement within an individual and across populations.<sup>19</sup> However, measurement of low abundance proteins using global proteomic methods still requires further optimization, and reported correlations between targeted and global analyses are less well-established.<sup>15,19</sup>

We aimed in this study to quantify a wide range of proteins relevant to the fate of drugs in humans. To our knowledge, the current report represents the most comprehensive analysis of the abundance of drug metabolizing enzymes, particularly, CYPs and UGTs, and drug transporters in human liver microsomal fractions to date using a label-free quantitative proteomic approach. This systematic study allows the evaluation of the global proteomic profile of the samples as well. This allowed an assessment of the purity of the microsomal samples. In addition, we were able to investigate the implication of the dynamic range of the proteome on the comparative analysis of protein abundance between individuals, and correlations between protein abundance and *in vitro* enzymatic activity and demographic characteristics.

## MATERIALS AND METHODS

**Chemicals.** Unless otherwise indicated, all chemicals were supplied by Sigma-Aldrich (Poole, Dorset, U.K.) with the highest purity available. Sequencing grade modified trypsin was supplied by Promega (Southampton, U.K.). All solvents were

HPLC grade and supplied by ThermoFisher Scientific (Paisley, U.K.).

**Human Liver Microsomal Samples.** Human liver microsomes (HLMs) from nontumorous liver samples ( $n = 23$ ) were provided by Pfizer (Groton, CT, USA). Suppliers of these samples were Vitron (Tucson, AZ, USA) and BD Gentest (San Jose, CA, USA). Demographic (ethnicity, age, and gender), clinical (medical history, medications, smoking history, and alcohol consumption), and genotype information on these donors were also provided by Pfizer (Supplementary Table 1). The 23 donors (10 females, 13 males) had an average age of 48.7 years (range 27–66 years) and an average BMI of  $29.7 \text{ kg m}^{-2}$  (range  $18.0\text{--}39.6 \text{ kg m}^{-2}$ ), including 9 overweight and 9 obese donors. Ethical approval was obtained by the suppliers, and the sample donors were anonymized. These samples have previously been analyzed by targeted quantitative proteomics.<sup>10,11,20</sup> In the present study, label-free quantification was applied to these samples according to the workflow shown in Supplementary Figure 1. Liver microsomal fractions were prepared using differential centrifugation methodology as previously described.<sup>21</sup> Briefly, low speed centrifugation (10000g) was performed to separate cellular debris from the crude cytosolic fraction made up of cytosolic components and low weight organelles. High speed centrifugation (100000g) was performed to pellet the microsomal fraction.

**Protein Content Quantification and Sample Preparation.** Protein content in the HLM samples was estimated by a spectrophotometric protein assay using the Bradford reagent (ThermoFisher Scientific, Hemel Hempstead, UK).<sup>22</sup> Analysis was made in triplicate according to the manufacturer's protocol using bovine serum albumin (BSA) as a standard. Microsomal fractions from 23 individuals were selected in this study. To enable absolute quantification by mass spectrometry,  $100 \mu\text{g}$  of each HLM fraction was spiked with an internal standard protein mixture containing  $0.3 \mu\text{g}$  of equine myoglobin,  $0.15 \mu\text{g}$  of bovine cytochrome *c*, and  $0.2 \mu\text{g}$  of BSA. These nonhuman proteins were selected because their low similarity with their human counterparts minimizes interference. To each fraction containing the standards, sodium deoxycholate was added to achieve a final concentration of 10% (w/v). The mixture was mixed well and incubated at room temperature for 10 min.

For protein digestion, a the filter-aided sample preparation (FASP) method was used as previously described with minor modifications, in order to optimize for microsomal samples.<sup>14,23</sup> Before sample addition, Amicon Ultra 0.5 mL centrifugal filters at 3 kDa molecular weight cutoff Merck Millipore, Nottingham, U.K.) were conditioned by briefly centrifuging  $400 \mu\text{L}$  of 60% (v/v) methanol at 14000g at room temperature. The deoxycholate-solubilized HLM samples were then transferred to the conditioned filter units. A final concentration of 100 mM 1,4-dithiothreitol (DTT) was added to the protein mixture, which was incubated at  $56^\circ\text{C}$  for 40 min. Following incubation, the samples were centrifuged at 14000g at room temperature for 20 min. Alkylation was performed with 50 mM iodoacetamide in the dark for 30 min at room temperature.

After alkylation, deoxycholate removal was performed by buffer exchange using two successive washes with 8 M urea in 100 mM Tris-HCl (pH 8.5). To reduce urea concentration, three additional washes were performed using 1 M urea in 50 mM ammonium bicarbonate (pH 8.5). Protein digestion was

achieved by adding trypsin (trypsin/protein ratio 1:25) followed by overnight incubation at 37 °C. Peptides were recovered by centrifugation (14000g, 20 min) first by elution using 100 mM ammonium bicarbonate (pH 8.5) followed by a second elution using 0.5 M sodium chloride. The eluted peptides were dried in a vacuum concentrator. The dried peptides were resuspended in loading buffer (3% (v/v) acetonitrile in water with 0.1% (v/v) trifluoroacetic acid) and desalted using a C18 column (Nest group, USA). The peptides were again dried using a vacuum concentrator and stored at -20 °C until mass spectrometric analysis.

**Liquid Chromatography and Tandem Mass Spectrometry (LC-MS/MS).** Dried peptide samples were resuspended in 100  $\mu$ L of loading buffer, and 1.0  $\mu$ L of each sample was loaded on an UltiMate 3000 rapid separation liquid chromatography (RSLC; Dionex, Surrey, U.K.) coupled to an online Q Exactive HF Hybrid Quadrupole-Orbitrap mass spectrometer (ThermoFisher Scientific, Bremen, Germany). The samples were analyzed in analytical duplicates (46 runs in total). Peptides were reversed-phase separated on a PepMap RSLC C18 column (2  $\mu$ m particles, 100 Å, 75  $\mu$ m inner diameter, 50 cm length) (Thermo Scientific, U.K.) preceded by a C18 PepMap100  $\mu$ -precursor column (5  $\mu$ m, 100 Å, 300  $\mu$ m inner diameter, 5 mm length) (ThermoFisher Scientific, UK). A multistep gradient was used from 4% to 40% buffer B (80% (v/v) acetonitrile with 0.1% (v/v) formic acid) for 100 min at a flow rate of 300 nL min<sup>-1</sup>. The composition of buffer A was HPLC grade water containing 0.1% (v/v) formic acid. The sensitivity and *m/z* accuracy of the mass spectrometer was evaluated using a positive ion calibration solution (ThermoFisher Scientific, Paisley, U.K.). The performance of the liquid chromatographer and mass spectrometer was evaluated using HeLa protein digest standard (ThermoFisher Scientific, Paisley, U.K.) over a 90 min gradient. Data were acquired in the positive ion mode in a data-dependent manner alternating between survey MS and MS/MS scans. MS scans were performed over the range of 100–1500 *m/z*, with 60 000 resolution, automatic gain control (AGC) of  $3 \times 10^6$ , and 100 ms maximal injection time. The top 18 precursor ions were sequentially selected for fragmentation using higher-energy collisional dissociation (HCD) with 28% normalized collision energy and precursor isolation window of 1.2 *m/z*. MS/MS scans were acquired at 30 000 resolution, AGC of  $5 \times 10^4$ , and 120 ms maximal injection time. Dynamic exclusion was set to 30 s.

**LC-MS/MS Data Analysis.** Protein and peptide identification and quantification were performed using Progenesis v4.0 (Nonlinear Dynamics, Newcastle-upon-Tyne, U.K.) and Mascot (Matrix Science, London, U.K.). The Progenesis software was used for precursor ion alignment based on retention time. Following precursor alignment, data were exported as Mascot generic files (mgf), and subsequently proteins were identified using Mascot. Proteins were identified by searching against a reference human proteome database containing 71 599 entries (UniProt, May 2017). Using Mascot, the precursor mass tolerance was set to 5 ppm, fragment mass tolerance was set to 0.5 Da, cysteine carbamidomethylation was considered as fixed modification, and oxidation of methionine and deamidation of asparagine/glutamine were considered as variable modifications. Trypsin was set as the proteolytic enzyme, and one missed cleavage was allowed. The list of identified proteins was imported back into Progenesis, and the identified proteins were matched with their abundance

quantified using BSA as the internal standard of choice. Among the three proteins used as internal standards, BSA was selected because the amount of BSA spiked in to each sample was empirically in the right dynamic range of the proteins of interest. The abundance of each relevant protein was quantified by the “Hi-N” method.<sup>24</sup> In this method, the peak intensity associated with the *N* most abundant nonconflicting peptide ions was automatically selected for quantification. The mean value of the intensities of the three most intense unique peptides of the protein of interest relative to the internal standard was used for the calculation of the proportionality factor.<sup>24</sup> The abundance of the protein of interest was calculated by multiplying the proportionality factor of each protein by the known abundance of BSA. Progenesis, in common with other mass spectrometry software, often identifies as “unique” peptides that are actually present in more than one cytochrome P450 or UGT enzyme. To overcome this limitation, the uniqueness of peptides from CYPs and UGTs was analyzed using *p*BLAST search (NCBI, USA). The abundance of each CYP and UGT protein detected in the HLM samples was recalculated manually using the unique peptides identified using *p*BLAST. The abundance was expressed in units of pmol mg<sup>-1</sup> microsomal protein.

**Protein Subcellular Localization and Annotation of Enzymes and Transporters.** To assess the purity and makeup of the microsomal fractions, the subcellular localization of all identified proteins (*n* = 2208) was annotated according to three databases, Gene Ontology (GO), UniProt, and the Human Protein Atlas (HPA), by searching the gene names against these repositories. Where there was evidence of expression in more than one subcellular component, the protein was assigned to all relevant localizations. The identified enzymes and transporters were checked for evidence of expression in hepatic tissue at both the RNA and protein levels against the NCBI human database and HPA; only hepatic proteins were included in subsequent analysis. In addition, the role of hepatic enzymes and transporters was identified using UniProt and NCBI databases, leading to selection of proteins involved in xenobiotic or drug metabolism and disposition. Only drug metabolizing enzymes and drug transporters quantifiable in at least one-third of the samples (*n*  $\geq$  7) were considered for subsequent statistical analysis.

**Cross-Methodology Assessment of Measured Enzyme Abundance Levels.** To establish the accuracy of the developed label-free assay, the abundance levels of enzymes measured in this study were compared to previously determined concentrations in matched samples using two targeted proteomic methodologies, QconCAT in the case of CYPs<sup>11</sup> and UGTs<sup>25</sup> and AQUA in the case of UGTs.<sup>10</sup>

**Assessment of CYP and UGT Abundance against Enzymatic Activity.** To validate the proteomic method, assessment of direct correlation between the quantified abundance of major drug metabolizing CYPs and UGTs and their enzymatic activity was performed. Metabolite appearance rates for CYPs (1A2, 2B6, 2C9, 2C19, 2D6, 3A4, and 3A5) and for UGTs (1A1, 1A3, 1A4, 1A6, 1A9, 2B4, 2B7, and 2B15) in these samples were kindly provided by Pfizer (Groton, CT, USA). Cytochrome P450 substrates<sup>26</sup> were phenacetin (CYP1A2), bupropion (CYP2B6), diclofenac (CYP2C9), S-mephenytoin (CYP2C19), bufuralol (CYP2D6), and testosterone (CYP3A4). CYP3A5 activity was measured using midazolam in the presence of a CYP3Cide to silence CYP3A4.<sup>27</sup> UGT substrates<sup>20,28</sup> were  $\beta$ -estradiol (UGT1A1),

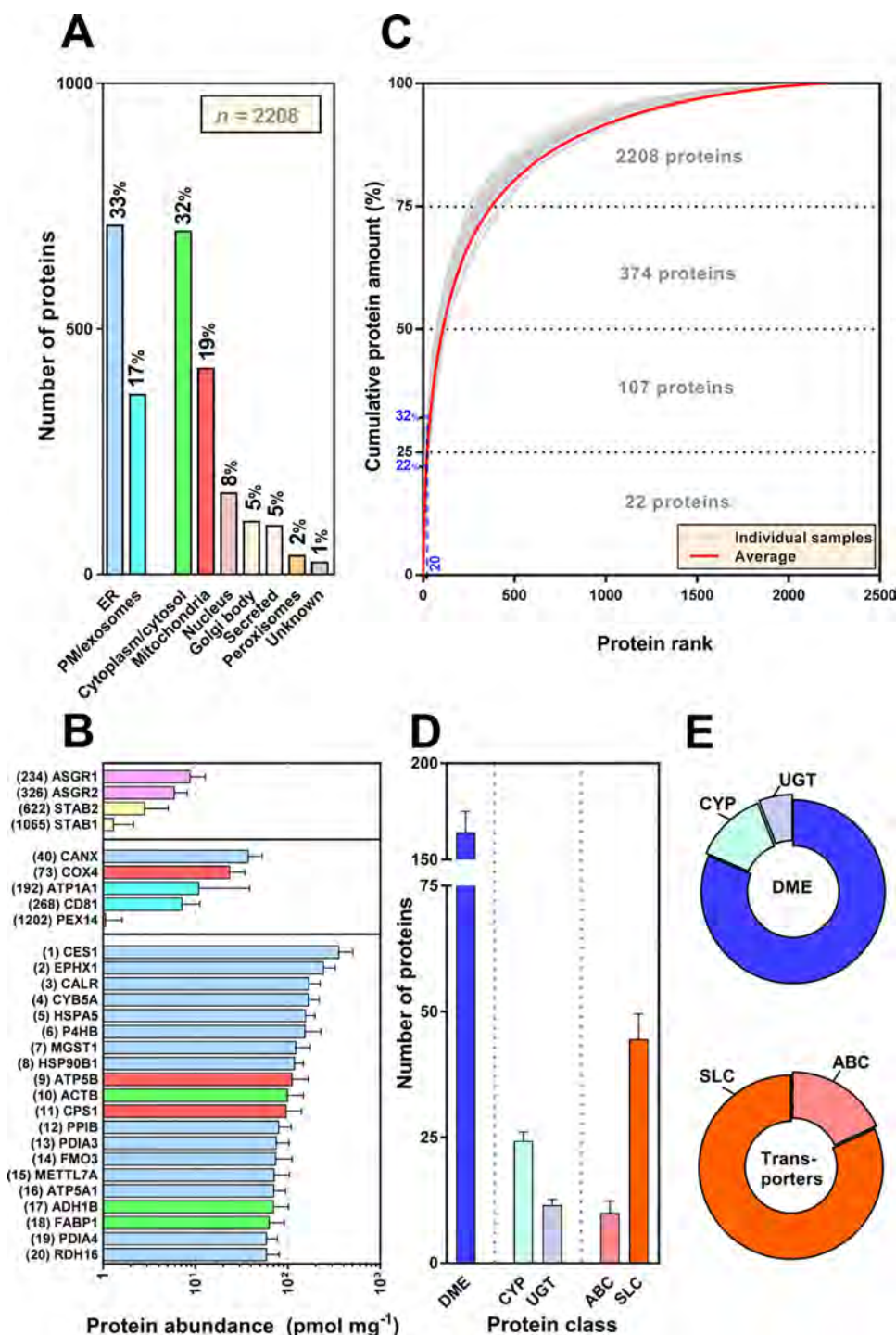


**Figure 1.** Global proteomic analysis of human liver microsomes ( $n = 23$  samples), showing the subcellular localization of identified proteins (A) and the origin of the 20 most abundantly expressed proteins mapped along with cell and organelle markers (B), showing that this fraction is contaminated due to the presence of different cell types (cell markers: ASGR1/2, hepatocytes; STAB1/2, liver endothelial cells) and cosedimentation of several cellular components (organelle markers: CANX, endoplasmic reticulum; ATP1A1/CD81, plasma membrane; COX4, mitochondria; PEX14, peroxisomes); the 20 most abundant proteins were of three origins, reticular, mitochondrial, and cytoplasmic/cytosolic. The cumulative amount of the quantified proteins (C), representing assessment of purity of the microsomal fraction, shows contribution of the 20 most highly abundant proteins to total protein amount (22%–32%). A large number of drug and xenobiotic metabolizing and transporting proteins were identified in the HLM samples (D), among which cytochrome P450 enzymes, UGTs, ATP-binding cassette (ABC), and solute carrier (SLC) transporters (E) are of particular interest. In panel A, the numbers of proteins in each subcellular component is shown along with percentage contribution to the total number of proteins; these percentages add up to more than 100% due to expression of several proteins in more than one subcellular location. ABC, ATP-binding cassette transporters; CYP, cytochrome P450 enzymes; DME, drug/xenobiotic metabolizing enzymes; ER, endoplasmic reticulum; PM, plasma membrane; SLC, solute carrier transporters; UGT, uridine 5'-diphospho-glucuronosyltransferases.

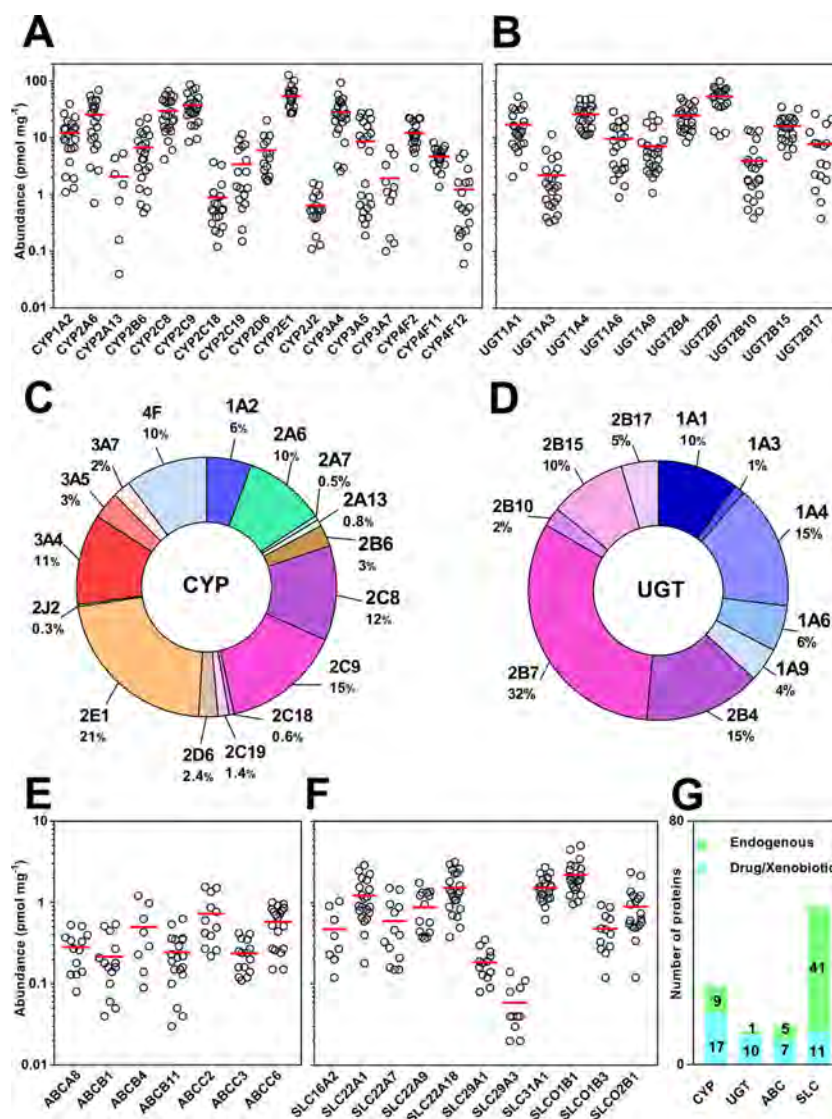


**Figure 2.** Scatter plots and pie charts representing the abundance of drug-metabolizing cytochrome P450 (A, C) and UGT (B, D) enzymes, scatter plots of the abundance of ABC (E) and SLC (F) drug transporters, and bar chart of the numbers of quantified enzymes and transporters involved in the metabolism and transport of drugs and endogenous compounds (G). In panels A, B, E, and F, the red bars represent mean abundance levels expressed in picomoles per milligram of microsomal protein. In panel G, CYP, cytochrome P450 enzymes; UGT, uridine *S'*-diphosphoglucuronosyltransferases; ABC, ATP-binding cassette transporters; SLC, solute carrier transporters; drug and endogenous refer to substrates of enzymes and transporters.

chenodeoxycholic acid (UGT1A3), trifluoperazine (UGT1A4), 5-hydroxytryptophol (UGT1A6), propofol (UGT1A9), zidovudine (UGT2B7), and *S*-oxazepam (UGT2B15).

**Statistical Analysis.** All statistical analysis of the data was performed using Microsoft Excel 2010, GraphPad Prism v7.03 (La Jolla California, USA), and R v3.4.3. Nonparametric statistics were used since a considerable proportion of the data set did not follow normal distribution. The normality of data distribution was assessed using three tests: D'Agostino–Pearson, Shapiro–Wilk, and Kolmogorov–Sminov normality tests. The Spearman rank-order correlation ( $R_s$ ) test, with  $t$ -distribution of the  $p$ -values, was used to assess enzyme abundance–activity correlation and intercorrelation between protein abundance levels. The level of scatter of data was evaluated by linear regression ( $R^2$ ). The relationship between age and expression level was also assessed using these correlation tests. Differences between abundances generated

by targeted (QconCAT/AQUA) and label-free methods were assessed using Mann–Whitney  $U$ -test and Kolmogorov–Sminov cumulative distribution test. Bias and scatter of the label free, AQUA, and QconCAT data sets were assessed using average fold error (AFE) and absolute average fold error (AAFE), respectively. Differences between genotypes and BMI categories were assessed using nonparametric Kruskal–Wallis ANOVA followed by post hoc Mann–Whitney  $U$ -test. The  $p$ -value cutoff for statistical significance was set at 0.05, which was Bonferroni-corrected when iterative tests were required to generate correlation matrices. Hierarchical cluster analysis (HCA) and principal components analysis (PCA) were performed using proteome-wide similarity data based on percentage identical peptide (PIP) and percentage identical protein (PIPr)<sup>23</sup> values across the 23 samples. Graphs were generated using GraphPad Prism v7.03 and R v3.4.3.

**Table 1. Expression Levels of 17 CYP Enzymes, NADPH-Cytochrome P450 Reductase (POR), and Cytochrome-b<sub>5</sub> (CYB5A) with Known Involvement in Drug Modification Pathways in Human Liver Microsomal Fractions<sup>a</sup>**

enzyme	median (pmol mg <sup>-1</sup> )	MAD <sup>b</sup> (pmol mg <sup>-1</sup> )	mean ± SD <sup>c</sup> (pmol mg <sup>-1</sup> )	CV <sup>d</sup> (%)	range (min–max) (pmol mg <sup>-1</sup> )	n <sup>e</sup>
CYP1A2	11.31	4.80	14.14 ± 13.02	92.08	1.11–56.42	23
CYP2A6	23.19	13.80	25.62 ± 19.41	75.78	0.71–69.68	21
<i>CYP2A13</i>	<i>1.50</i>	<i>0.80</i>	<i>2.07 ± 2.07</i>	<i>100.15</i>	<i>0.04–5.32</i>	7
CYP2B6	5.36	3.40	6.78 ± 5.99	88.41	0.48–22.63	23
CYP2C8	24.59	15.90	29.78 ± 18.65	62.61	4.18–67.52	23
CYP2C9	32.60	10.60	37.53 ± 20.67	55.08	8.49–87.20	23
CYP2C18	0.55	0.30	1.60 ± 2.44	152.83	0.12–9.66	20
CYP2C19	1.38	1.10	3.43 ± 3.59	104.49	0.15–11.62	17
CYP2D6	4.44	2.40	6.05 ± 5.11	84.49	1.74–20.54	15
CYP2E1	50.69	15.00	54.38 ± 24.67	45.36	26.94–127.26	23
CYP2J2	0.53	0.10	0.64 ± 0.43	66.97	0.11–1.59	17
CYP3A4	25.46	11.20	28.52 ± 20.67	72.47	2.58–93.71	23
CYP3A5	5.80	5.20	8.63 ± 9.51	110.24	0.19–27.78	23
CYP3A7	1.35	1.30	5.54 ± 9.63	173.80	0.10–33.73	13
CYP4F2	10.97	2.60	12.22 ± 5.74	46.99	2.98–22.36	23
CYP4F11	4.54	1.10	5.06 ± 2.47	48.86	1.37–13.69	23
<i>CYP4F12</i>	<i>0.58</i>	<i>0.45</i>	<i>1.23 ± 1.51</i>	<i>122.27</i>	<i>0.06–5.27</i>	18
CYB5A <sup>f</sup>	160.05	23.40	169.19 ± 49.63	29.33	88.69–260.67	23
POR <sup>f</sup>	38.86	10.10	41.17 ± 14.20	34.49	18.53–74.73	23

<sup>a</sup>Protein expression is represented by the median, the median absolute deviation (MAD), the mean, the standard deviation of the mean (SD), the coefficient of variation (CV), and the range (min–max). Proteins highlighted in italic have been quantified for the first time in this study. Abundance of CYPs is expressed in pmol mg<sup>-1</sup> of liver microsomal protein. <sup>b</sup>Median absolute deviation is a nonparametric measure of variability around the median. <sup>c</sup>Standard deviation describes variability around the mean where data is expected to be extracted from a normally distributed population. SD describes both technical and biological variability. <sup>d</sup>Coefficient of variation calculated as a percentage ( $CV = SD_i/\bar{x}_i$ ) for each enzyme *i*. <sup>e</sup>Number of human liver microsomal samples. <sup>f</sup>Cytochrome P450 auxiliary proteins.

## RESULTS

**General Outcome.** Across the twenty-three liver microsomal fractions, a total of 2208 proteins were quantified with a minimum of two unique peptides each and a false discovery rate of ≤1% at the protein and peptide levels. In each sample, an average of 1994 proteins was quantified (range 1836–2152 proteins). The present study represents an increase of approximately 30% of ADME proteins quantified in liver microsomal samples when compared with previously reported data.<sup>15,29</sup>

**Evaluation of the Reproducibility of the Proteomics Data.** Analytical replicates were evaluated in two ways. First, high reproducibility was seen in the quantified abundance of identical proteins across analytical replicates as the coefficient of determination from regression analysis ( $R^2$ ) varied between 0.79 and 0.99, with a slope of approximately one. In addition, categorical evidence was used to assess the similarity between peptides identified in the analytical replicates at the level of the primary analytes (peptides) using the descriptor percentage identical peptides (PIP) as previously described.<sup>23</sup> In each sample, a very high similarity was seen in the peptides identified in the analytical replicates with PIP varying between 92% and 100%. The details of replicate evaluation are provided in [Supplementary Table 2](#). Values in this range point to a high degree of consistency in both sample preparation and instrument performance and are reassuring, especially in view of the long mass spectrometry run required by 23 samples in duplicate.

**Assessment of the Quality of Liver Microsomal Fractions.** Subcellular localization analysis of the samples predicted that approximately 50% of the quantified proteins were localized in the endoplasmic reticulum and the plasma membrane. The remaining proteins were largely predicted to

be localized in the cytoplasm or cytosol, the mitochondria, and the nucleus ([Figure 1A](#)). This prediction was confirmed by the presence of markers specific for these organelles. Although calnexin (CANX), the specific marker for endoplasmic reticulum membrane, was abundant in the global microsomal protein profile, markers for mitochondrial membrane (cytochrome *c* oxidase; COX4), plasma membrane (sodium/potassium-transporting ATPase subunit alpha-1 and cluster of differentiation 81; ATP1A1 and CD81) and peroxisomal membrane (peroxisomal membrane protein; PEX14) were also present ([Figure 1B](#)).<sup>30–32</sup> Established protein markers for hepatocytes, asialoglycoprotein receptor 1 (ASGR1) and asialoglycoprotein receptor 2 (ASGR2), were highly expressed in the microsomal preparation,<sup>33,34</sup> but markers specific to nonparenchymal endothelial cells (stabilin 1 and 2; STAB1/2) were also present, indicating some heterogeneity of cell type.<sup>35</sup> Markers associated with other cell types such as Kupffer cells, Ito cells, and intrahepatic cholangiocytes were not found. The heterogeneity of the microsomal samples makes this analysis especially important, as variation in contamination would have a profound effect on the apparent abundance of proteins involved in drug metabolism and transport when expressed as pmol of protein per microgram of microsomal protein, as is conventional.<sup>29,36,37</sup>

An analysis of the 20 most abundant proteins across all microsomal fractions was undertaken to determine whether the contaminants could affect the quantification of proteins in the microsomal fractions. In this study, 15 out of the 20 most abundant proteins quantified in the microsomal fractions were predicted to be localized in the endoplasmic reticulum ([Figure 1B](#)). The most abundant protein in all microsomal fractions was either liver carboxylesterase 1 (CES1) or epoxide hydrolase 1 (EPHX1), both reticular proteins, at average

**Table 2. Expression Levels of 10 UGT Enzymes with Known Involvement in Drug Glucuronidation in Human Liver Microsomal Fractions<sup>a</sup>**

enzyme	median (pmol mg <sup>-1</sup> )	MAD <sup>b</sup> (pmol mg <sup>-1</sup> )	mean ± SD <sup>c</sup> (pmol mg <sup>-1</sup> )	CV <sup>d</sup> (%)	range (min–max) (pmol mg <sup>-1</sup> )	n <sup>e</sup>
UGT1A1	12.29	4.60	17.13 ± 12.81	74.79	2.08–53.64	23
UGT1A3	1.36	0.80	2.21 ± 2.55	115.72	0.33–11.58	23
UGT1A4	22.70	8.90	26.06 ± 12.41	47.63	11.18–49.88	23
UGT1A6	7.89	5.50	9.64 ± 7.69	79.81	0.90–29.10	23
UGT1A9	5.19	2.40	7.18 ± 6.47	90.13	1.07–25.00	23
UGT2B4	24.57	10.10	24.64 ± 12.06	48.95	8.36–50.58	23
UGT2B7	56.17	14.90	53.97 ± 22.84	42.31	10.86–100.37	23
UGT2B10	1.92	1.40	3.99 ± 4.29	107.71	0.39–13.84	23
UGT2B15	15.42	5.60	16.18 ± 7.85	48.54	4.80–35.12	23
UGT2B17	5.43	3.45	7.81 ± 7.93	101.47	0.38–26.50	16

<sup>a</sup>Protein expression is represented by the median, the median absolute deviation (MAD), the mean, the standard deviation of the mean (SD), the coefficient of variation (CV), and the range (min–max). Abundance of UGTs is expressed in pmol mg<sup>-1</sup> of liver microsomal protein. <sup>b</sup>Median absolute deviation is a nonparametric measure of variability around the median. <sup>c</sup>Standard deviation describes variability around the mean where data is expected to be extracted from a normally distributed population. SD describes both technical and biological variability. <sup>d</sup>Coefficient of variation calculated as a percentage ( $CV = SD_i/\bar{x}_i$ ) for each enzyme *i*. <sup>e</sup>Number of human liver microsomal samples.

**Table 3. Expression Levels of 18 Transporters with Known Involvement in Drug Clearance in Human Liver Microsomal Fractions<sup>a</sup>**

transporter	median (pmol mg <sup>-1</sup> )	MAD <sup>b</sup> (pmol mg <sup>-1</sup> )	mean ± SD <sup>c</sup> (pmol mg <sup>-1</sup> )	CV <sup>d</sup> (%)	range (min–max) (pmol mg <sup>-1</sup> )	n <sup>e</sup>
ATP-Binding Cassette Transporters						
ABCA8	0.27	0.10	0.28 ± 0.15	51.96	0.08–0.53	13
ABCB1	0.18	0.09	0.47 ± 0.77	162.43	0.04–2.95	16
ABCB4	0.36	0.25	0.50 ± 0.41	81.92	0.09–1.21	8
ABCB11	0.22	0.13	0.28 ± 0.21	76.26	0.03–0.90	21
ABCC2	0.54	0.25	0.73 ± 0.49	67.93	0.22–1.55	12
ABCC3	0.25	0.10	0.74 ± 1.40	188.35	0.11–5.42	18
ABCC6	0.70	0.30	1.02 ± 1.47	145.01	0.15–6.60	21
Solute Carrier Transporters						
<i>SLC16A2</i>	0.33	0.20	0.47 ± 0.35	73.27	0.12–1.04	8
<i>SLC22A1</i>	1.02	0.40	1.35 ± 0.93	69.19	0.18–4.09	22
<i>SLC22A7</i>	0.43	0.25	0.79 ± 0.87	110.53	0.15–3.36	14
<i>SLC22A9</i>	0.77	0.35	0.88 ± 0.48	54.35	0.36–1.75	14
<i>SLC22A18</i>	1.31	0.50	1.52 ± 0.82	54.04	0.38–3.15	21
<i>SLC29A1</i>	0.18	0.10	0.18 ± 0.08	43.49	0.08–0.35	13
<i>SLC31A1</i>	1.46	0.40	1.61 ± 0.69	42.72	0.62–3.62	21
<i>SLC29A3</i>	0.04	0.02	0.06 ± 0.04	66.02	0.02–0.14	11
SLCO1B1	1.98	0.60	2.45 ± 1.59	64.65	0.96–8.04	23
SLCO1B3	0.47	0.20	0.77 ± 0.83	107.93	0.12–3.25	14
SLCO2B1	0.63	0.30	0.89 ± 0.58	65.08	0.12–2.36	19

<sup>a</sup>Protein expression is represented by the median, the median absolute deviation (MAD), the mean, the standard deviation of the mean (SD), the coefficient of variation (CV), and the range (min–max). Proteins highlighted in italic have been quantified for the first time in this study. Abundance of transporters is expressed in pmol mg<sup>-1</sup> of liver microsomal protein. <sup>b</sup>Median absolute deviation is a nonparametric measure of variability around the median. <sup>c</sup>Standard deviation describes variability around the mean where data is expected to be extracted from a normally distributed population. SD describes both technical and biological variability. <sup>d</sup>Coefficient of variation calculated as a percentage ( $CV = SD_i/\bar{x}_i$ ) for each enzyme *i*. <sup>e</sup>Number of human liver microsomal samples.

concentrations of 360 and 247 pmol mg<sup>-1</sup> liver microsomal protein, respectively. The 20 most abundant proteins constituted 22%–32% (average 24%) of the quantified microsomal fraction (Figure 1C).

**Assessment of the Abundance of Cytochrome P450 and Uridine 5'-Diphosphate-Glucuronosyltransferase UGT Enzymes and Drug Transporters.** Cytochrome P450 (CYP) and uridine 5'-diphosphate-glucuronosyltransferase (UGT) enzymes are the principal enzymes responsible for the metabolism of drugs and xenobiotics. Of these, 188 enzymes and 66 transporters were quantified in at least seven individuals as shown in Supplementary Tables 8–11. These include 26 CYPs, 11 UGTs, 12 ABC transporters, and 52 SLC

transporters (Figure 1D,E). Of the quantified CYPs, UGTs and transporters, 17 CYPs, 10 UGTs, 7 ABC transporters and 11 SLC transporters are known to be associated with drug clearance based on pharmacological and toxicological evidence. Hepatic microsomal abundance levels of these enzymes and transporters are shown in Figure 2 and summarized in Tables 1–3. Where literature values were available, they were compared with the present study and found to be in broad agreement (Supplementary Tables 4–7). The most highly expressed CYPs were CYP2E1, CYP2C9, CYP2C8, CYP3A4, and CYP2A6 (Figure 2A).<sup>6,38–40</sup> The most highly expressed UGT was UGT2B7, followed by UGT1A4, UGT2B4, UGT1A1, and UGT2B15 (Figure 2B). The pie charts in

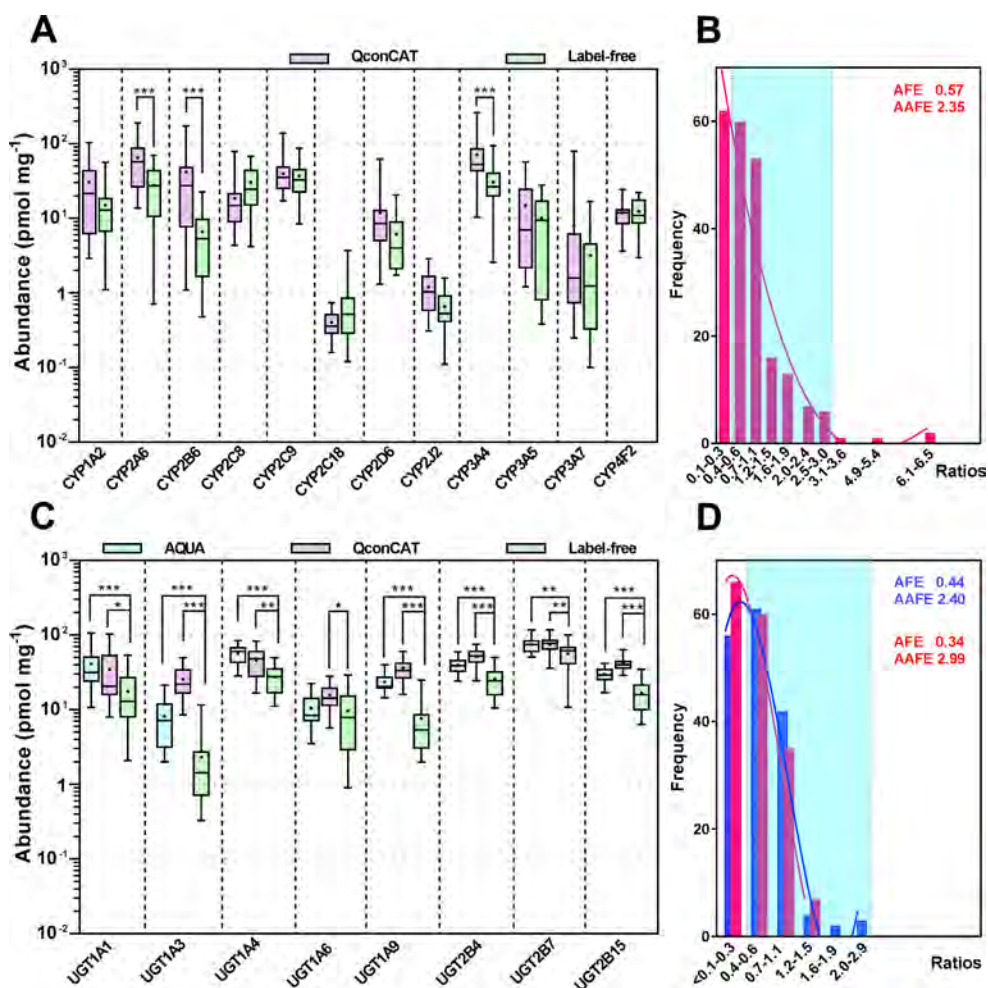


**Figure 3.** Comparison of abundance values measured using the label-free strategy relative to two targeted methods (AQUA and QconCAT) for cytochrome P450 enzymes (A, B) and UDP-glucuronosyltransferases (C, D) in matched liver microsomal samples ( $n = 21$ ). In panels A and C, enzyme abundances are shown as box and whiskers plots with the whiskers representing the ranges, the boxes representing the 25th and 75th percentiles, the lines showing the medians, and the + signs denoting the means. Mann–Whitney tests were used to assess differences with statistically significant discrepancies shown; \* $P < 0.05$ ; \*\* $P < 0.01$ ; \*\*\* $P < 0.001$ . In panels B and D, fold error values are plotted as a frequency distribution showing lower values generated by label-free quantification. Fold errors are calculated as  $x_1/x_2$  ratios for label free measurements ( $x_1$ ) relative to targeted measurements ( $x_2$ ) using either QconCAT (C) or AQUA and QconCAT (D). The light-blue shaded area indicates values within 3-fold, considered as generally interchangeable. AFE, average fold error; AAFE, absolute average fold error; abundance levels are expressed in picomoles per milligram of HLM protein.

Figure 2C,D show the relative abundance distribution of CYPs and UGTs involved in drug metabolism in the liver, which are very similar to distributions reported in recent data analysis.<sup>41,42</sup>

The most abundant ABC transporter is ABCC6 (Figure 2E) and SLCO1B1 is the most abundant transporter in the human liver (Figure 2F).<sup>6</sup> Although we successfully quantified ABCB5, ABCG8, and SLC47A1, the expression levels of these enzymes are not reported in Figure 2E,F and Table 3 as these proteins were quantified in fewer than seven individuals. Enzymes and transporters involved in the metabolism and clearance of endogenous compounds were also quantified, including 9 CYPs, 1 UGT, 5 ABC transporters, and 41 SLC transporters (Figure 2G). Individual data for all enzymes and transporters quantified in this study are provided in Supplementary Tables 8–11. The abundance of enzymes and transporters was measured in units of pmol mg<sup>-1</sup> microsomal protein.

### Comparison of CYP and UGT Abundance in Label-Free and Targeted Proteomics Measurements.

The HLM fractions here analyzed by the label-free approach have previously been used to quantify the abundance of CYP and UGT enzymes using targeted proteomic approaches,<sup>10,11</sup> presenting a unique opportunity for comparison of these proteomic workflows. The CYP enzymes have previously been quantified using a QconCAT-based strategy,<sup>9</sup> in which labeled standard peptides are concatenated together in an artificial protein and released by tryptic digestion. The UGTs have also been quantified by targeted approach but using individual isotopic-labeled (AQUA) peptides as standards.<sup>8</sup>

Comparison of the median and distribution of CYP abundances quantified previously by the targeted QconCAT strategy<sup>11</sup> with the label-free approach used in this study indicated that there was very good agreement between the studies across most of the quantified CYP enzymes, with less good but still reasonable agreement for CYP2A6, CYP2B6, and CYP3A4 (Figure 3A and Supplementary Figure 2). Analysis

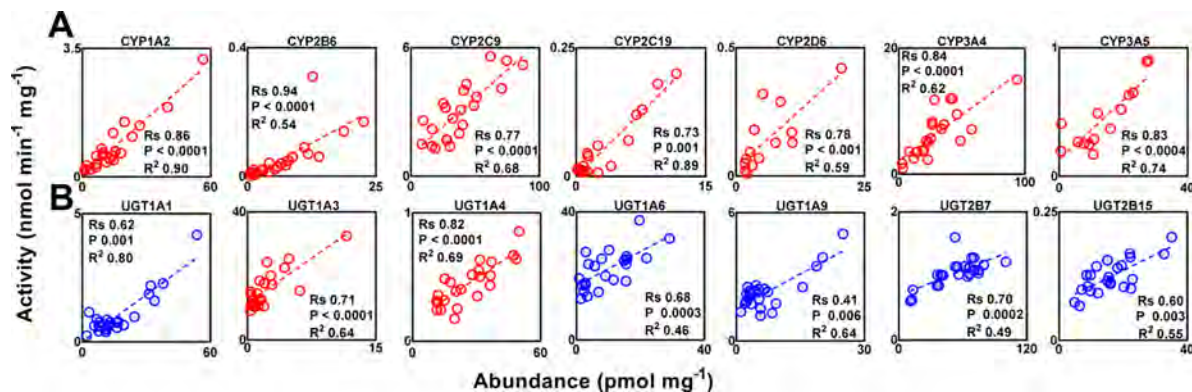


**Figure 4.** Correlation of the abundance levels of cytochrome P450 (A) and uridine 5'-diphospho-glucuronosyltransferase enzymes (B) measured using label-free global proteomics against catalytic activity. Strong and significant correlations ( $R_s > 0.70$ ,  $P < 0.008$ ) with very limited scatter ( $R^2 > 0.50$ ) are shown in red; moderate correlations ( $R_s > 0.50$ ,  $P < 0.008$ ) with limited scatter ( $R^2 > 0.30$ ) are shown in blue. CYP substrates: CYP1A2 (phenacetin), CYP2B6 (bupropion), CYP2C9 (diclofenac), CYP2C19 (*S*-mephenytoin), CYP2D6 (bufuralol), CYP3A4 (testosterone), CYP3A5 (midazolam). UGT substrates: UGT1A1 ( $\beta$ -estradiol), UGT1A3 (chenodeoxycholic acid), UGT1A4 (trifluoperazine), UGT1A6 (*S*-hydroxytryptophol), UGT1A9 (propofol), UGT2B7 (zidovudine), UGT2B15 (*S*-oxazepam). Abundance is measured in units of picomole per milligram of microsomal protein, and activity is measured in units of nanomole per minute per milligram of microsomal protein. The CYP3A5 activity was measured in the presence of a CYP3A4 inhibitor to silence CYP3A4.

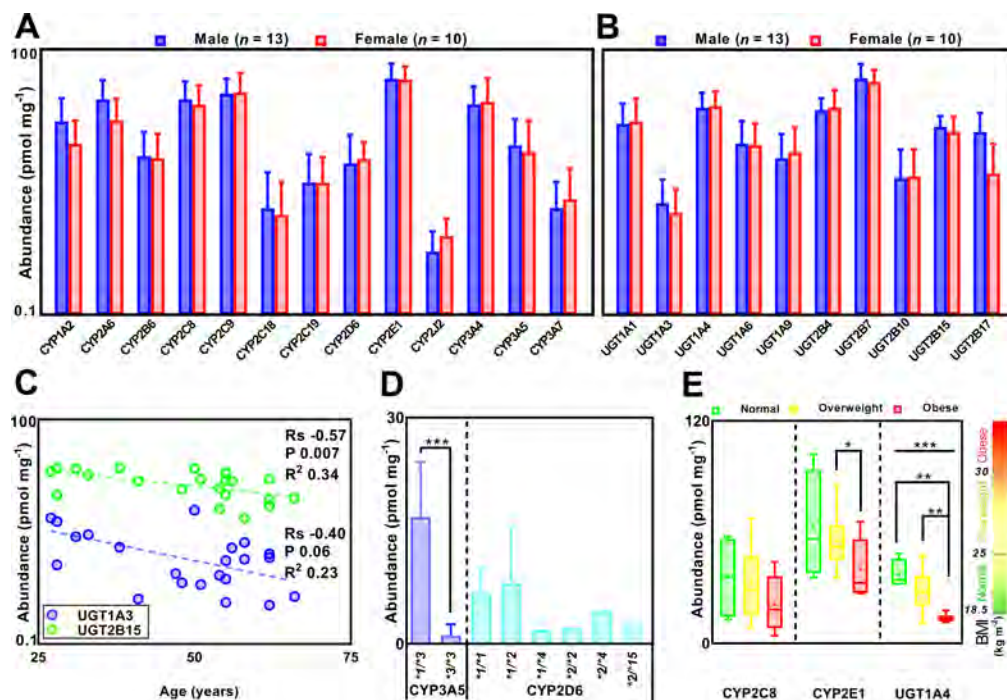


**Figure 5.** Covariates of expression of hepatic cytochrome P450 and UGT enzymes measured using the label-free proteomic strategy. The variables assessed were sex (A, B), age (C), genotype (D), and body mass index, BMI (E). Sex did not affect expression with no significant differences between male and female donors (A and B). An overall declining trend with age was observed for all enzymes, with little statistical significance except for a few UGT examples (C). Genotype was a significant factor for CYP3A5 expression with \*1/\*3 genotype being expressed at higher levels than \*3/\*3 (16-fold higher). Only borderline significant difference in expression was seen between CYP2D6 genotypes (C). There was an overall declining trend of expression with BMI with differences of expression observed between normal weight, overweight, and moderately obese patients (D) assessed using ANOVA and Mann–Whitney test for group and pairwise analysis. In panels A, B, and D, abundance data are presented as mean  $\pm$  SD. In panel C,  $R_s$  is Spearman rank-order correlation coefficient. In panel E, the boxes are the 25th and 75th percentiles, the whiskers are the ranges, the lines are the medians, and the + signs are the means. The scale inset on the right is the BMI scale for the three categories (normal BMI 18.5–25; overweight BMI 25–30; obese BMI > 30  $\text{kg m}^{-2}$ ); \* $P < 0.05$ ; \*\* $P < 0.01$ ; \*\*\* $P < 0.001$ .

of fold-errors for individual microsomal samples assessed using the developed method relative to the targeted approach revealed that approximately 70% of the values generated by the two methods were within 3-fold<sup>20</sup> and 21% of values were within the bioequivalence range (80%–125%).<sup>43</sup> Both bias (indicated by a value of the average fold error, AFE, different

from 1) and scatter (indicated by an absolute average fold error, AAFE, higher than 1) were observed (Figure 3B).

UGT enzymes had previously been quantified by two targeted approaches, based on AQUA and QconCAT standards (Figure 3C Supplementary Figure 2). The quantification of UGTs is extremely challenging because of

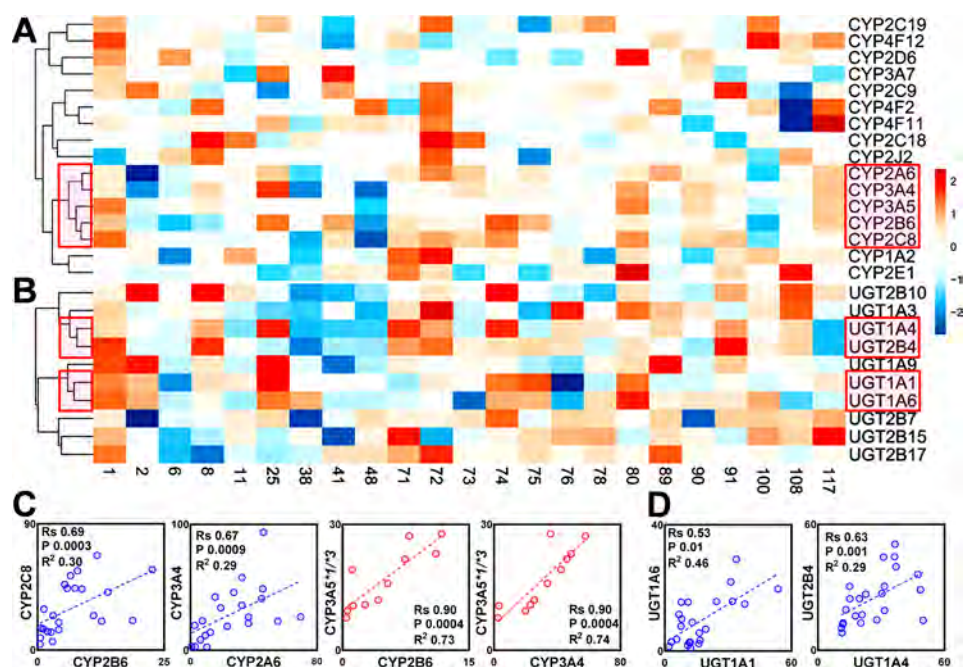


**Figure 6.** Heat maps showing the abundance levels of drug metabolizing cytochrome P450 (A) and UDP-glucuronosyltransferase (B) enzymes in the microsomal samples. Cluster generation was based on rank-order correlation of normal log-transformed expression data. Blue shows low abundances and red high abundances. The red shaded boxes denote the main correlation clusters in the two enzyme families. Examples of significant correlations within CYP and UGT data are shown in panels C and D, respectively. Strong correlations are shown in red and moderate ones in blue. Correlation statistics are provided in [Supporting Information](#). Abundance levels are expressed in picomole per milligram of HLM protein.

(a) the very low abundance of some of these proteins, (b) the fact that they are membrane-bound, and (c) the shared peptide sequences between UGTs, and hence, the difficulty in identifying unique peptides. Overall the present experiments reported lower abundances for the UGTs than either of the targeted methods, although again the values determined here fell within the range of UGT abundance reported in the literature ([Supplementary Table 5](#)) and a large proportion (approximately 64%) of values were within 3-fold, with a smaller proportion (17%) within the bioequivalence range.<sup>20,43</sup> [Figure 3D](#) shows the presence of both bias and scatter when the methods were compared.

**Correlation between CYPs and UGTs Protein Expression and Enzymatic Activity.** The correlation between protein abundance quantified by the label-free approach and *in vitro* enzymatic activity was assessed for all CYP and UGT enzymes for which activity data were available. Correlations were deemed strong when the values correlated well ( $R_s > 0.60$  with statistical significance against a Benferroni-corrected cutoff  $p$ -value) and demonstrated limited scatter ( $R^2 > 0.30$ ). The results demonstrated strong, significant, and positive correlation between abundance and enzymatic activity across all CYP enzymes ([Figure 4A](#)). These correlations are better than those observed in a previous study using a targeted QconCAT strategy,<sup>11</sup> thus highlighting the importance of the selection of peptide for quantification ([Supplementary Tables 13–15](#)). Strong positive correlation between protein abundance and enzymatic activity was also seen for two UGT enzymes, UGT1A3 and UGT1A4, with moderate positive correlation for the remaining UGT enzymes ([Figure 4B](#)). These correlations are comparable with those observed using a targeted AQUA strategy,<sup>20</sup> which assessed correlation in a

larger sample size ( $n = 59$ ) compared to the current study ( $n = 23$ ).

**Covariates of Expression of Liver Enzymes and Transporters.** Trends in the expression of enzymes and transporters were assessed with reference to several factors, including sex, age, genotype, smoking, alcohol consumption, and body mass index (BMI) of donors. Demographic and clinical information on donors is provided in [Supplementary Table 1](#). There were no significant differences in expression of enzymes between male and female donors ([Figure 5A,B](#)); the seemingly higher levels of CYP3A4 and 3A7 in female donors did not reach statistical significance (Mann–Whitney  $U$ -test,  $P > 0.05$ ). A declining trend of expression with age was observed for enzymes and transporters, which did not reach statistical significance due to extensive scatter of the data, except for a few examples, including UGT2B15 ([Figure 5C](#)). Smoking and drinking did not seem to affect expression of enzymes; however, the number of smokers ( $n = 4$ ) and regular alcohol consumers ( $n = 3$ ) among the donors was very low for statistical assessment. The effect of genotype on expression was demonstrated by CYP3A5, with 16-fold higher levels (Mann–Whitney  $U$ -test,  $P < 0.001$ ) observed with \*1/\*3 genotype compared to its mostly inactive \*3/\*3 counterpart ([Figure 5D](#)). The effect of BMI was assessed in three categories (healthy weight, BMI 18.5–25 kg m<sup>-2</sup>; overweight, 25–30 kg m<sup>-2</sup>; and obese >30 kg m<sup>-2</sup>), and expression of enzymes and transporters tended to decline with increasing BMI ([Figure 5E](#)). Nonparametric (Kruskal–Wallis) ANOVA showed differences with borderline statistical significance for CYP2E1 ( $P = 0.08$ ) and statistically significant differences for UGTs 1A3, 1A4, and 2B10, and transporters SLC27A2 and SLC27A5 ( $P < 0.05$ ). Post hoc Mann–Whitney  $U$ -test showed statistically significant differences between BMI categories for CYP2E1,

UGTs 1A3, 1A4, and 2B10, and SLCs 27A2 and 27A5 ( $P < 0.05$ ). The average age for the three categories was 42.3, 46.1, and 55.4 years, so the effect of BMI may have been confounded by age.

**Correlations of Expression between Hepatic Drug-Metabolizing Enzymes and Transporters.** Patterns in the expression of enzymes and transporters were also assessed for potential intercorrelation at the protein level. The heat map in Figure 6 shows normal log-transformed abundance levels of cytochrome P450 enzymes (Figure 6A) and UGT enzymes (Figure 6B). The clustering method was based on rank-order correlation. Examples of correlations in the CYP and UGT data sets are shown in Figure 6C,D, respectively. Observed intercorrelations between CYP enzymes included CYP2C8/CYP2B6 ( $R_s = 0.69$ ,  $P = 0.0003$ ;  $R^2 = 0.30$ ); CYP3A4/CYP3A5\*1/\*3 ( $R_s = 0.90$ ,  $P = 0.0004$ ;  $R^2 = 0.74$ ) and CYP2A6/CYP3A4 ( $R_s = 0.67$ ,  $P = 0.0009$ ;  $R^2 = 0.29$ ). UGT correlations included UGT1A4/UGT1A9 ( $R_s = 0.63$ ,  $P = 0.001$ ;  $R^2 = 0.23$ ) and UGT1A4/UGT2B4 ( $R_s = 0.63$ ,  $P = 0.001$ ;  $R^2 = 0.29$ ). Cross-family correlations were overall weak-to-moderate and included CYP3A4/UGT1A1 ( $R_s = 0.53$ ,  $P = 0.01$ ;  $R^2 = 0.40$ ), which was previously reported to be moderate in a targeted experiment.<sup>11</sup> These correlations are related to common regulatory mechanisms of gene expression, and the findings of this study are confirmatory of previously reported correlations.<sup>9,11</sup>

Intercorrelations between hepatic drug transporters included ABCC2/ABCC3 ( $R_s = 0.81$ ,  $P = 0.006$ ;  $R^2 = 0.12$ ); SLC29A1/SLC29A3 ( $R_s = 0.78$ ,  $P = 0.03$ ;  $R^2 = 0.48$ ) and ABCC6/SLC22A9 ( $R_s = 0.81$ ,  $P = 0.002$ ;  $R^2 = 0.54$ ). However, the number of sample pairs for strong and significant correlations was low ( $n = 7-12$ ), which may require confirmation with higher numbers of samples. Only one of the uncovered correlations, ABCC2/ABCC3, was previously reported to be strong.<sup>44</sup> Once confirmed, correlations of expression levels of enzymes and transporters can be used in more realistic simulations of drug clearance and drug-drug interactions, as demonstrated previously with several examples of CYP enzymes.<sup>45,46</sup>

**Evaluation of Similarity between Biological Samples.** Similarity between biological replicates of the 23 biological samples was also evaluated looking at the proteome profiles using PIP and percentage identical proteins (PIPr) for all pairs of samples, and the results are shown in Supplementary Figure 3. PIP varied between 41% and 66%, and PIPr varied between 70% and 83% (Supplementary Table 3). Given the consistency in the methodology used, these variations are likely to reflect biological differences. Supplementary Figure 3 shows cluster analysis of data at both the peptide and protein levels, suggesting agreement between peptide and protein data, with two distinct clusters identified by hierarchical cluster analysis (HCA) and principal components analysis (PCA). The data form two clusters, but the relationship between the members of the clusters is, at this stage, unclear. There was no clear correlation with demographic and clinical data; although the small cluster contains largely younger, healthier individuals who were not taking any medication.

## DISCUSSION

In contrast to targeted proteomics where only a predefined set of proteins can be quantified, label-free proteomics allows us to simultaneously quantify a large subset of the proteome in an individual, leading to a systems-level understanding of the

cellular physiology. However, obtaining reproducible and accurate results using the label-free approach requires mass spectrometers capable of delivering high mass accuracy, liquid chromatography platforms able to deliver highly reproducible retention times, and sophisticated software able to minimize technical variability by allowing accurate retention time alignment between multiple runs.<sup>17,18</sup> In this study, the use of modern instrumentation with the above-mentioned capabilities along with improvements in sample preparation has allowed the quantification of more than 2200 proteins in human liver microsomes including 45 proteins involved in the metabolism and transport of drugs and other xenobiotics. CYPs and UGTs are the proteins primarily involved in drug metabolism in the human liver. In this study, several CYPs and UGTs were found in the human liver microsomes. In agreement with published data, the highly expressed CYPs were CYP2E1, CYP2C9, CYP2C8, CYP3A4, and CYP2A6.<sup>6,38-40</sup> In this study, CYP3A43, a well-known drug-metabolizing enzyme, was also measured but only in fewer than seven individuals. In agreement with published data, the most highly expressed UGT was UGT2B7, followed by UGT1A4, UGT2B4, UGT1A1, and UGT2B15.<sup>6-10,38,39</sup> Where literature data are available, the quantification of the ABC and SLC transporters in this study is also in agreement.<sup>15,47,48</sup>

A number of drug metabolizing enzymes (CYPs 2A13 and 4F12) and drug transporters (SLCs 16A2, 22A18, 29A3, and 31A1) were quantified for the first time. CYP2A13 is responsible for metabolic activation of many tobacco-specific carcinogens and similarly to CYP1A2 can also metabolize 4-aminobiphenyl, phenacetin, and aflatoxin B1.<sup>49</sup> CYP4F12 can metabolize arachidonic acid and ebastine.<sup>50</sup> SLC16A2 is known to have a profound physiological role in thyroid hormone transport and specific substrates for this transporter are thyroxine, diiodothyronine, and triiodothyronine.<sup>51</sup> SLC22A18 has a role in the transport of chloroquine and quinidine-related compounds.<sup>52</sup> SLC31A1 is a copper transporter that mediates the flux of cisplatin and other platinum anticancer drugs.<sup>53</sup> Finally, SLC29A3 is a transporter involved in mediating equilibrative diffusion of nucleoside drugs, such as cladribine, fludarabine, cytarabine, and gemcitabine, across the plasma membrane.<sup>54</sup> The ability to quantify novel targets such as those reported in this study is one of the primary advantages of label-free quantification methodology.

In some previous studies, CYP4A11 was included in the quantified drug metabolizing enzymes,<sup>6,15</sup> mainly because polymorphisms in CYP4A11 have been associated with hypertension/cardiovascular disease, which can have an effect on choice of therapeutic drugs.<sup>55</sup> In this study, although CYP4A11 was successfully quantified, it was not considered to be a drug metabolizing enzyme. We also quantified several proteins the polymorphisms of which are associated with several diseases, such as UGT1A1 (Gilbert's syndrome) and ABCC2 (Dubin-Johnson syndrome), which in turn could affect the choice of therapeutic drugs prescribed. Some examples of proteins involved in disease development are shown in Supplementary Tables 8 (CYPs), 9 (UGTs), 10 (ABC transporters), and 11 (SLC transporters). However, further evaluation of these proteins is beyond the scope of this study.

The human liver microsomal samples used in this study have previously been used to quantify CYPs and UGTs using targeted proteomics approaches. Overall, there was good

agreement in protein abundance measurements between the label-free approach used in the present study and the previous targeted proteomic approaches; nonetheless, the results are not identical. This can be due to several factors. First, label-free quantification assumes a uniform correlation between peptide peak intensity and its abundance, which is not true since different peptides present at the same concentration generate mass spectrometric signals of different intensities.<sup>12</sup> The Hi-3 method can theoretically offset peptide-specific bias to some degree by using the median of the three most intense signals for each protein. Taking this into account, in contrast to targeted proteomics, label-free analysis is not intrinsically an absolute quantification strategy. Second, differences in abundance of proteins quantified using label-free and targeted proteomics may be affected by the proteins and peptides used as standards for quantification. In particular, the choice of signature peptides for targeted quantification of CYP, UGT, and transporter proteins is challenging and relies on stringent criteria. We compared the peptides used for label-free analysis with those used for targeted quantification (where available), and there was limited overlap between the two sets (Supplementary Tables 13–15). In addition, appraisal of the set of peptides used for the global analysis indicated their suitability as surrogates. Most importantly, the discrepancies in observed protein abundances may well be driven by differences in workflows used for sample preparation (Supplementary Table 17) with no consensus on standardized methodology. In studies involving drug metabolism in the liver, protein abundances obtained from mass spectrometric analysis are normalized to the mass of liver microsomal fractions. However, the purity of microsomal fractions is not typically reported, which makes interlaboratory comparisons of results quite challenging. Although only 19% of the results were within the bioequivalence range of 0.8- to 1.25-fold,<sup>43</sup> which is extremely strict for this purpose, in the majority of cases (67% of all ratios), the two methods yielded a fold difference of less than 3.<sup>20</sup> Analysis of the AFE and AAFE showed that the untargeted methodology gives systematically lower results than the targeted methods for UGTs but not for CYPs. In principle, we would expect targeted methodology to yield more accurate quantification, because the standards are simple isotopomers of the peptides being assessed, whereas untargeted methods rely on medians of dissimilar standards. In practice, poor choice of standards, transitions, or molar ratio of standard to sample can compromise targeted measurements, and only the last of these applies to untargeted experiments. Both sets of measurements show good agreement with activity data, but the activity data is not based on absolute amounts of enzymes (CYPs or UGTs) so cannot be used to arbitrate between the proteomics measurements. Nevertheless, assessment of correlations between protein abundances estimated by the label-free and targeted approaches indicated that the data were generally well-correlated, as shown in Supplementary Table 16.

The real advantage of label-free measurements, especially when acquired using state-of-the-art mass spectrometry, is that a very large number of proteins may be quantified simultaneously. The additional proteins include markers of different cell types and cellular components, enabling an assessment of the purity of biological samples not immediately available by other methods. Human liver microsomes were, until recently, thought to be composed predominantly of endoplasmic reticulum from the parenchymal hepatocytes.<sup>56</sup> Discrepancies in the total number detected in liver systems, as

reported previously,<sup>15</sup> may well be due to the nature of the system being analyzed, with analyses of whole cell lysates generally identifying higher numbers of proteins compared to enriched fractions, such as microsomes. Other differences can be attributed to several methodological factors that can affect every step of the experimental workflow. Recently, it has been shown that microsomal fractions are typically heterogeneous, enriching endoplasmic reticulum but also proteins from other cellular compartments.<sup>29</sup> The reliability of quantification of proteins of interest may therefore be compromised by variability in the levels of nonreticular proteins. On the positive side, the contamination by other cell types and cellular components was very consistent across these samples, ranging from 22% to 32%. Label-free methodology is expected to be particularly powerful when microsomal preparations from different sources are compared. Cytosolic enzymes involved in drug-metabolism (e.g., sulfotransferases or glutathione transferases) were also detected in the microsomal fractions; however, since the cytosol represents a contaminant to microsomal preparations, these abundance data should be established in a more representative fraction, such as, cytosol or homogenate, in order for these data to be used in systems pharmacology modeling and extrapolation exercises.

Drug-metabolizing enzymes and transporters have historically been quantified in units of picomole per milligram of microsomal protein. This is also the case in this manuscript. We have previously shown that varying expression of the most abundant proteins can affect the apparent abundance of the proteins involved in drug metabolism and transport, when expressed as picomole of protein per milligram of microsomal protein.<sup>29,37,57</sup> We and others have therefore advocated the use of picomole per gram of tissue as a way of overcoming the effects of the most abundant proteins in the human liver microsomes on absolute quantification of the abundance of drug metabolizing enzymes and transporters.<sup>29,37,57</sup> The present study points to a still more important reason for a change in unit, the possibility of varying amounts of contamination. There are, of course, limitations to using tissue mass as a standard for these measurements, although the literature is encouraging.

Simulations of drug trials rely on the use of scaling factors, including abundance levels, with realistic variability and correlations with clinical and demographic factors.<sup>5</sup> Our data revealed large levels of interindividual variation across CYP enzymes (4–340-fold), UGT enzymes (5–70-fold), ABC transporters (7–200-fold), and SLC transporters (4–27-fold), highlighting the importance of elucidating and incorporating sources of variability. There were no significant sex-related differences in abundance of enzymes and transporters, consistent with a recent meta-analysis of CYP protein abundance.<sup>42</sup> The overall trend of age-related decline in enzyme and transporter levels, although with no statistical significance in most cases, seemed to be a consistent observation, which requires further confirmation. The effect of age after maturation of expression has previously been reported to be minimal on abundance and activity of CYP enzymes per mass of liver.<sup>58–60</sup> However, *in vivo* metabolic ratios analysis showed a decrease in whole liver metabolic capacity with age, mirroring the decline in renal function.<sup>61</sup> These two observations can be explained by a decline in liver size to match body size decrease in older adults,<sup>62</sup> accompanied by a decrease in the amount of liver protein per gram of liver.<sup>63</sup> Therefore, although the abundance levels

normalized to microsomal protein content seem minimally affected, there are indications that whole liver content of such enzymes and transporters may be affected. This finding is corroborated by reduced drug hepatic clearance observed in older patients.<sup>64</sup>

Out of all the factors examined, genotype is perhaps the most clinically recognized covariate of expression and activity. The data in this study confirmed previously highlighted genotype-specific differences in the expression of CYP3A5<sup>11,65</sup> and CYP2D6.<sup>66</sup> These differences in expression are expected to propagate to differences in enzymatic activity and therefore hepatic clearance of substrate drugs of these enzymes. In addition, our data suggest that higher body mass index (BMI) is consistent with a decline in the expression of enzymes and transporters, in line with recent evidence.<sup>67</sup> This observation is consistent with the pro-inflammatory effect of obesity leading to decreased enzymatic and transporter activity.<sup>68</sup> The analyzed set of samples was mostly from older obese or overweight donors, which should be considered when using the generated data.

Although information related to expression covariates has the potential to improve the accuracy of predicting drug clearance and drug–drug interactions, it can be argued that these factors are still not utilized effectively. This highlights the importance of collecting data on very well-characterized populations, such as the present data set. Another very useful aspect of abundance data that has recently been incorporated into modeling exercises is intercorrelations between individual proteins.<sup>45,46</sup> The data set uncovered several correlations that can be used to build more realistic systems pharmacology models, including the intercorrelations CYP3A4/CYP3A5\*1/\*3,<sup>45</sup> UGT1A4/UGT2B4,<sup>69</sup> and ABCC2/ABCC3.<sup>44</sup> These can also be confirmed at the mRNA level,<sup>70,71</sup> which further supports reports of common genetic regulation of expression of enzymes and transporters. It has been reported that drug transporter abundances quantified in microsomal fractions are frequently overestimated. To overcome this problem, the relative expression scaling factor (REF), which accounts for the differences between the abundance of drug transporters in microsomal fractions and those in human hepatocytes, has been used to improve the accuracy of *in vivo* drug clearance for *in vitro*–*in vivo* extrapolation.<sup>36</sup> Such approaches, when established, should enable more realistic predictions of the outcomes of therapy and better design of dosage regimens.<sup>29</sup>

## CONCLUSIONS

We describe a label-free proteomic approach for the quantification of drug-metabolizing enzymes and transporters in liver, based on high resolution mass spectrometry and rigorous data analysis. Validity of the data was confirmed against targeted proteomic data in matched samples and against enzyme catalytic activity. The method provides highly comprehensive information that can be used to ascertain the quality of samples, describe expression covariates, and cluster donors based on the primary analytes. The information obtained generally complements that of targeted proteomics, and the label-free approach enabled quantification of two drug-metabolizing enzymes and four transporters for the first time. The pattern of expression supports the view that genotype, age, and obesity (but not gender) affect the expression of several drug-metabolizing enzymes and transporters. We expect that the use of this versatile label-free quantification approach will increase the availability of accurate and comprehensive protein

abundance information, which will enhance prediction of drug efficacy and safety using computational models. This in turn will enable the optimization of dosage of medicines given to patients to achieve maximal drug efficacy with limited toxicity. Considering the many existing gaps in QSP models, label-free proteomics offers a fast solution for simultaneous quantification of a wide range of proteins as the first step, which can, in time, be complemented by more targeted measurements.

## ASSOCIATED CONTENT

### Supporting Information

The Supporting Information is available free of charge on the ACS Publications website at DOI: 10.1021/acs.molpharmaceut.8b00941.

Demographic and clinical information from the liver donors, reproducibility data, comparative information on targeted and label-free proteomics for CYPs, UGTs, and transporters, label-free quantification information for all identified CYPs, UGTs, and transporters, a compilation of sample preparation and analytical procedures used in different laboratories, pictorial representation of the experimental workflow, and principal component analysis data of biological reproducibility using PIP and PIPr (PDF)

## AUTHOR INFORMATION

### Corresponding Authors

\*E-mail: [narciso.couto@manchester.ac.uk](mailto:narciso.couto@manchester.ac.uk).

\*E-mail: [jill.barber@manchester.ac.uk](mailto:jill.barber@manchester.ac.uk).

### ORCID

Narciso Couto: 0000-0001-7565-4357

Zubida M. Al-Majdoub: 0000-0002-1497-3140

Brahim Achour: 0000-0002-2595-5626

### Present Address

<sup>||</sup>P.C.W.: School of Engineering, Faculty of Science, Agriculture & Engineering, Newcastle University, Newcastle upon Tyne, NE1 7RU, UK.

### Author Contributions

<sup>†</sup>N.C. and Z.M.A.-M. contributed equally to this work. This study was conceived by N.C., Z.M.A.-M., and J.B. N.C. and Z.M.A.-M. performed the experiments. Data analysis was performed by N.C., Z.M.A.-M., B.A., and J.B. All authors contributed to the writing of the manuscript.

### Notes

The authors declare no competing financial interest.

## ACKNOWLEDGMENTS

The authors thank Pfizer (Groton, CT) for providing HLM samples along with demographic, clinical, and enzymatic activity data, the ChELSI Institute, University of Sheffield, for access to LC-MS/MS instrumentation (funded under BBSRC grant BB/M012166/1 and EPSRC grant EP/E036252/1), and the Bio-MS core facility, University of Manchester, for access to Progenesis software. We also thank Dr. Anna Vildhede (AstraZeneca) for providing label-free data from her study.

## ABBREVIATIONS

ABC, ATP-binding cassette; ADME, absorption, distribution, metabolism, and elimination; AQUA, absolute quantification; BSA, bovine serum albumin; CYP, cytochrome P450; DDI,

drug–drug interaction; FASP, filter-aided sample preparation; HLM, human liver microsome; IVIVE, *in vitro*–*in vivo* extrapolation; LC-MS/MS, liquid chromatography–tandem mass spectrometry; PBPK, physiologically based pharmacokinetics; QconCAT, quantification concatemer; SLC, solute carrier; UGT, uridine 5′-diphosphate-glucuronosyltransferase; UPLC, ultraperformance liquid chromatography

## REFERENCES

- (1) Jamei, M. Recent Advances in Development and Application of Physiologically-Based Pharmacokinetic (PBPK) Models: A Transition from Academic Curiosity to Regulatory Acceptance. *Current Pharmacology Reports* **2016**, *2*, 161–169.
- (2) Rostami-Hodjegan, A. Physiologically Based Pharmacokinetics Joined With In Vitro–In Vivo Extrapolation of ADME: A Marriage Under the Arch of Systems Pharmacology. *Clin. Pharmacol. Ther.* **2012**, *92* (1), 50–61.
- (3) FDA Program of physiologically-based pharmacokinetic and pharmacodynamic modeling (PBPK Program), 2018.
- (4) Turner, R. M.; Park, B. K.; Pirmohamed, M. Parsing Interindividual Drug Variability: An Emerging Role for Systems Pharmacology. *Wiley Interdisciplinary Reviews: Systems Biology and Medicine* **2015**, *7*, 221–241.
- (5) Rostami-Hodjegan, A.; Tucker, G. T. Simulation and Prediction of *in Vivo* Drug Metabolism in Human Populations from *in Vitro* Data. *Nat. Rev. Drug Discovery* **2007**, *6*, 140–148.
- (6) Ohtsuki, S.; Schaefer, O.; Kawakami, H.; Inoue, T.; Liehner, S.; Saito, A.; Ishiguro, N.; Kishimoto, W.; Ludwig-Schwellinger, E.; Ebner, T.; et al. Simultaneous Absolute Protein Quantification of Transporters, Cytochromes P450, and UDP-Glucuronosyltransferases as a Novel Approach for the Characterization of Individual Human Liver: Comparison with mRNA Levels and Activities. *Drug Metab. Dispos.* **2012**, *40* (1), 83–92.
- (7) Sato, Y.; Nagata, M.; Tetsuka, K.; Tamura, K.; Miyashita, A.; Kawamura, A.; Usui, T. Optimized Methods for Targeted Peptide-Based Quantification of Human Uridine 5′-Diphosphate-Glucuronosyltransferases in Biological Specimens Using Liquid Chromatography–Tandem Mass Spectrometry. *Drug Metab. Dispos.* **2014**, *42* (5), 885–889.
- (8) Harbourt, D. E.; Fallon, J. K.; Ito, S.; Baba, T.; Ritter, J. K.; Glish, G. L.; Smith, P. C. Quantification of Human Uridine-Diphosphate Glucuronosyl Transferase 1A Isoforms in Liver, Intestine, and Kidney Using Nanobore Liquid Chromatography–Tandem Mass Spectrometry. *Anal. Chem.* **2012**, *84* (1), 98–105.
- (9) Margailan, G.; Rouleau, M.; Klein, K.; Fallon, J. K.; Caron, P.; Villeneuve, L.; Smith, P. C.; Zanger, U. M.; Guillemette, C. Multiplexed Targeted Quantitative Proteomics Predicts Hepatic Glucuronidation Potential. *Drug Metab. Dispos.* **2015**, *43* (9), 1331–1335.
- (10) Fallon, J. K.; Neubert, H.; Hyland, R.; Goosen, T. C.; Smith, P. C. Targeted Quantitative Proteomics for the Analysis of 14 UGT1As and –2Bs in Human Liver Using NanoUPLC-MS/MS with Selected Reaction Monitoring. *J. Proteome Res.* **2013**, *12* (10), 4402–4413.
- (11) Achour, B.; Russell, M. R.; Barber, J.; Rostami-Hodjegan, A. Simultaneous Quantification of the Abundance of Several Cytochrome P450 and Uridine 5′-Diphosphate-Glucuronosyltransferase Enzymes in Human Liver Microsomes Using Multiplexed Targeted Proteomics. *Drug Metab. Dispos.* **2014**, *42* (4), 500–510.
- (12) Couto, N.; Barber, J.; Gaskell, S. J. Matrix-Assisted Laser Desorption/Ionisation Mass Spectrometric Response Factors of Peptides Generated Using Different Proteolytic Enzymes. *J. Mass Spectrom.* **2011**, *46* (12), 1233–1240.
- (13) Wegler, C.; Gaugaz, F. Z.; Andersson, T. B.; Wiśniewski, J. R.; Busch, D.; Gröer, C.; Oswald, S.; Norén, A.; Weiss, F.; Hammer, H. S.; et al. Variability in Mass Spectrometry-Based Quantification of Clinically Relevant Drug Transporters and Drug Metabolizing Enzymes. *Mol. Pharmaceutics* **2017**, *14* (9), 3142–3151.
- (14) Wiśniewski, J. R.; Zougman, A.; Nagaraj, N.; Mann, M. Universal Sample Preparation Method for Proteome Analysis. *Nat. Methods* **2009**, *6* (5), 359–362.
- (15) Vildhede, A.; Wiśniewski, J. R.; Norén, A.; Karlgren, M.; Artursson, P. Comparative Proteomic Analysis of Human Liver Tissue and Isolated Hepatocytes with a Focus on Proteins Determining Drug Exposure. *J. Proteome Res.* **2015**, *14* (8), 3305–3314.
- (16) Al Feteisi, H.; Achour, B.; Barber, J.; Rostami-Hodjegan, A. Choice of LC-MS Methods for the Absolute Quantification of Drug-Metabolizing Enzymes and Transporters in Human Tissue: A Comparative Cost Analysis. *AAPS J.* **2015**, *17* (12), 438–446.
- (17) Neilson, K. A.; Ali, N. A.; Muralidharan, S.; Mirzaei, M.; Mariani, M.; Assadourian, G.; Lee, A.; Van Sluyter, S. C.; Haynes, P. A. Less Label, More Free: Approaches in Label-Free Quantitative Mass Spectrometry. *Proteomics* **2011**, *11* (4), 535–553.
- (18) Megger, D. A.; Bracht, T.; Meyer, H. E.; Sitek, B. Label-Free Quantification in Clinical Proteomics. *Biochim. Biophys. Acta, Proteins Proteomics* **2013**, *1834* (8), 1581–1590.
- (19) Wiśniewski, J. R.; Wegler, C.; Artursson, P. Multiple-Enzyme-Digestion Strategy Improves Accuracy and Sensitivity of Label- and Standard-Free Absolute Quantification to a Level That Is Achievable by Analysis with Stable Isotope-Labeled Standard Spiking. *J. Proteome Res.* **2018**, *18* (1), 217–224.
- (20) Achour, B.; Dantonio, A.; Niosi, M.; Novak, J. J.; Fallon, J. K.; Barber, J.; Smith, P. C.; Rostami-Hodjegan, A.; Goosen, T. C. Quantitative Characterization of Major Hepatic UDP-Glucuronosyltransferase Enzymes in Human Liver Microsomes: Comparison of Two Proteomic Methods and Correlation with Catalytic Activity. *Drug Metab. Dispos.* **2017**, *45* (10), 1102–1112.
- (21) Langenfeld, E.; Zanger, U. M.; Jung, K.; Meyer, H. E.; Marcus, K. Mass Spectrometry-Based Absolute Quantification of Microsomal Cytochrome P450 2D6 in Human Liver. *Proteomics* **2009**, *9* (9), 2313–2323.
- (22) Bradford, M. M. A Rapid and Sensitive Method for the Quantitation of Microgram Quantities of Protein Utilizing the Principle of Protein-Dye Binding. *Anal. Biochem.* **1976**, *72* (1–2), 248–254.
- (23) Al Feteisi, H.; Al-Majdoub, Z. M.; Achour, B.; Couto, N.; Rostami-Hodjegan, A.; Barber, J. Identification and Quantification of Blood-Brain Barrier Transporters in Isolated Rat Brain Microvessels. *J. Neurochem.* **2018**, *146* (6), 670–685.
- (24) Silva, J. C.; et al. Absolute Quantification of Proteins by LCMSE: A Virtue of Parallel Ms Acquisition. *Mol. Cell. Proteomics* **2006**, *5* (1), 144–156.
- (25) Achour, B.; Dantonio, A.; Niosi, M.; Novak, J. J.; Al-Majdoub, Z. M.; Goosen, T. C.; Rostami-Hodjegan, A.; Barber, J. Data Generated by Quantitative Liquid Chromatography–Mass Spectrometry Proteomics Are Only the Start and Not the Endpoint: Optimization of Quantitative Concatemer-Based Measurement of Hepatic Uridine-5′-Diphosphate–Glucuronosyltransferase Enzymes with Reference to Catalytic Activity. *Drug Metab. Dispos.* **2018**, *46* (6), 805–812.
- (26) Walsky, R. L.; Obach, R. S. Validated Assays for Human Cytochrome P450 Activities. *Drug Metab. Dispos.* **2004**, *32* (6), 647–660.
- (27) Walsky, R. L.; Obach, R. S.; Hyland, R.; Kang, P.; Zhou, S.; West, M.; Geoghegan, K. F.; Helal, C. J.; Walker, G. S.; Goosen, T. C.; et al. Selective Mechanism-Based Inactivation of CYP3A4 by CYP3Cide (PF-04981517) and Its Utility as an *in Vitro* Tool for Delineating the Relative Roles of CYP3A4 versus CYP3A5 in the Metabolism of Drugs. *Drug Metab. Dispos.* **2012**, *40* (9), 1686–1697.
- (28) Walsky, R. L.; Bauman, J. N.; Bourcier, K.; Giddens, G.; Lapham, K.; Neghaban, A.; Ryder, T. F.; Obach, R. S.; Hyland, R.; Goosen, T. C. Optimized Assays for Human UDP-Glucuronosyltransferase (UGT) Activities: Altered Alamethicin Concentration and Utility to Screen for UGT Inhibitors. *Drug Metab. Dispos.* **2012**, *40* (5), 1051–1065.
- (29) Achour, B.; Al Feteisi, H.; Lanucara, F.; Rostami-Hodjegan, A.; Barber, J. Global Proteomic Analysis of Human Liver Microsomes:

Rapid Characterization and Quantification of Hepatic Drug-Metabolizing Enzymes. *Drug Metab. Dispos.* **2017**, *45* (6), 666–675.

(30) Neufeld, C.; Filipp, F. V.; Simon, B.; Neuhaus, A.; Schüller, N.; David, C.; Kooshapur, H.; Madl, T.; Erdmann, R.; Schliebs, W.; et al. Structural Basis for Competitive Interactions of Pex14 with the Import Receptors Pex5 and Pex19. *EMBO J.* **2009**, *28* (6), 745–754.

(31) Rak, M.; Bénit, P.; Chrétien, D.; Bouchereau, J.; Schiff, M.; El-Khoury, R.; Tzagoloff, A.; Rustin, P. Mitochondrial Cytochrome c Oxidase Deficiency. *Clin. Sci.* **2016**, *130* (6), 393–407.

(32) Prior, K. K.; Wittig, I.; Leisegang, M. S.; Groenendyk, J.; Weissmann, N.; Michalak, M.; Jansen-Dürr, P.; Shah, A. M.; Brandes, R. P. The Endoplasmic Reticulum Chaperone Calnexin Is a NADPH Oxidase NOX4 Interacting Protein. *J. Biol. Chem.* **2016**, *291* (13), 7045–7059.

(33) Peters, D. T.; Henderson, C. A.; Warren, C. R.; Friesen, M.; Xia, F.; Becker, C. E.; Musunuru, K.; Cowan, C. A. Asialoglycoprotein Receptor 1 Is a Specific Cell-Surface Marker for Isolating Hepatocytes Derived from Human Pluripotent Stem Cells. *Development* **2016**, *143* (9), 1475–1481.

(34) Harris, R. L.; van den Berg, C. W.; Bowen, D. J. ASGR1 and ASGR2, the Genes That Encode the Asialoglycoprotein Receptor (Ashwell Receptor), Are Expressed in Peripheral Blood Monocytes and Show Interindividual Differences in Transcript Profile. *Mol. Biol. Int.* **2012**, *2012*, 1–10.

(35) Miller, C. M.; Donner, A. J.; Blank, E. E.; Egger, A. W.; Kellar, B. M.; Østergaard, M. E.; Seth, P. P.; Harris, E. N. Stabilin-1 and Stabilin-2 Are Specific Receptors for the Cellular Internalization of Phosphorothioate-Modified Antisense Oligonucleotides (ASOs) in the Liver. *Nucleic Acids Res.* **2016**, *44* (6), 2782–2794.

(36) Vildhede, A.; Nguyen, C.; Erickson, B. K.; Kunz, R. C.; Jones, R.; Kimoto, E.; Bourbonnais, F.; Rodrigues, A. D.; Varma, M. V. S. Comparison of Proteomic Quantification Approaches for Hepatic Drug Transporters: Multiplexed Global Quantitation Correlates with Targeted Proteomic Quantitation. *Drug Metab. Dispos.* **2018**, *46* (5), 692–696.

(37) Drozdik, M.; Busch, D.; Lapczuk, J.; Müller, J.; Ostrowski, M.; Kurzawski, M.; Oswald, S. Protein Abundance of Clinically Relevant Drug-Metabolizing Enzymes in the Human Liver and Intestine: A Comparative Analysis in Paired Tissue Specimens. *Clin. Pharmacol. Ther.* **2018**, *104* (3), 515–524.

(38) Achour, B.; Russell, M. R.; Barber, J.; Rostami-Hodjegan, A. Simultaneous Quantification of the Abundance of Several Cytochrome P450 and Uridine 5'-Diphospho-Glucuronosyltransferase Enzymes in Human Liver Microsomes Using Multiplexed Targeted Proteomics. *Drug Metab. Dispos.* **2014**, *42* (4), 500–510.

(39) Asha, S.; Vidyavathi, M. Role of Human Liver Microsomes in In Vitro Metabolism of Drugs—A Review. *Appl. Biochem. Biotechnol.* **2010**, *160* (6), 1699–1722.

(40) Zhang, H.-F.; Li, Z.-H.; Liu, J.-Y.; Liu, T.-T.; Wang, P.; Fang, Y.; Zhou, J.; Cui, M.-Z.; Gao, N.; Tian, X.; et al. Correlation of Cytochrome P450 Oxidoreductase Expression with the Expression of 10 Isoforms of Cytochrome P450 in Human Liver. *Drug Metab. Dispos.* **2016**, *44* (8), 1193–1200.

(41) Achour, B.; Rostami-Hodjegan, A.; Barber, J. Protein Expression of Various Hepatic Uridine 5'-Diphosphate Glucuronosyltransferase (UGT) Enzymes and Their Inter-Correlations: A Meta-Analysis. *Biopharm. Drug Dispos.* **2014**, *35* (6), 353–361.

(42) Achour, B.; Barber, J.; Rostami-Hodjegan, A. Expression of Hepatic Drug-Metabolizing Cytochrome P450 Enzymes and Their Intercorrelations: A Meta-Analysis. *Drug Metab. Dispos.* **2014**, *42* (8), 1349–1356.

(43) Davit, B. M.; Nwakama, P. E.; Buehler, G. J.; Conner, D. P.; Haidar, S. H.; Patel, D. T.; Yang, Y.; Yu, L. X.; Woodcock, J. Comparing Generic and Innovator Drugs: A Review of 12 Years of Bioequivalence Data from the United States Food and Drug Administration. *Ann. Pharmacother.* **2009**, *43* (10), 1583–1597.

(44) Mooij, M. G.; van de Steeg, E.; Van Rosmalen, J.; Windster, J. D.; de Koning, B. A. E.; Vaes, W. H.; van Groen, B. D.; Tibboel, D.; Wortelboer, H. M.; de Wildt, S. N. Proteomic Analysis of the

Developmental Trajectory of Human Hepatic Membrane Transporter Proteins in the First Three Months of Life. *Drug Metab. Dispos.* **2016**, *44*, 1005–1013.

(45) Barter, Z. E.; Perrett, H. F.; Yeo, K. R.; Allorge, D.; Lennard, M. S.; Rostami-Hodjegan, A. Determination of a Quantitative Relationship between Hepatic CYP3A5\*1/\*3 and CYP3A4 Expression for Use in the Prediction of Metabolic Clearance in Virtual Populations. *Biopharm. Drug Dispos.* **2010**, *31* (8–9), 516–532.

(46) Doki, K.; Darwich, A. S.; Achour, B.; Tornio, A.; Backman, J. T.; Rostami-Hodjegan, A. Implications of Intercorrelation between Hepatic CYP3A4-CYP2C8 Enzymes for the Evaluation of Drug-Drug Interactions: A Case Study with Repaglinide. *Br. J. Clin. Pharmacol.* **2018**, *84* (5), 972–986.

(47) Prasad, B.; Evers, R.; Gupta, A.; Hop, C. E. C. A.; Salphati, L.; Shukla, S.; Ambudkar, S. V.; Unadkat, J. D. Interindividual Variability in Hepatic Organic Anion-Transporting Polypeptides and P-Glycoprotein (ABCB1) Protein Expression: Quantification by Liquid Chromatography Tandem Mass Spectroscopy and Influence of Genotype, Age, and Sex. *Drug Metab. Dispos.* **2014**, *42* (1), 78–88.

(48) Fallon, J. K.; Smith, P. C.; Xia, C. Q.; Kim, M. S. Quantification of Four Efflux Drug Transporters in Liver and Kidney Across Species Using Targeted Quantitative Proteomics by Isotope Dilution NanoLC-MS/MS. *Pharm. Res.* **2016**, *33* (9), 2280–2288.

(49) Fukami, T.; et al. CYP2A13 Metabolizes the Substrates of Human CYP1A2, Phenacetin, and Theophylline. *Drug Metab. Dispos.* **2007**, *35* (3), 335–339.

(50) Hashizume, T. Involvement of CYP2J2 and CYP4F12 in the Metabolism of Ebastine in Human Intestinal Microsomes. *J. Pharmacol. Exp. Ther.* **2002**, *300* (1), 298–304.

(51) Bernal, J.; Guadaño-Ferraz, A.; Morte, B. Thyroid Hormone Transporters-Functions and Clinical Implications. *Nat. Rev. Endocrinol.* **2015**, *11* (7), 406–417.

(52) Ito, S.; Fujino, Y.; Ogata, S.; Hirayama-Kurogi, M.; Ohtsuki, S. Involvement of an Orphan Transporter, SLC22A18, in Cell Growth and Drug Resistance of Human Breast Cancer MCF7 Cells. *J. Pharm. Sci.* **2018**, *107* (12), 3163–3170.

(53) Fung, K. L.; Tepede, A. K.; Pluchino, K. M.; Pouliot, L. M.; Pixley, J. N.; Hall, M. D.; Gottesman, M. M. Uptake of Compounds That Selectively Kill Multidrug-Resistant Cells: The Copper Transporter SLC31A1 (CTR1) Increases Cellular Accumulation of the Thiosemicarbazone NSC73306. *Mol. Pharmaceutics* **2014**, *11* (8), 2692–2702.

(54) King, A. E.; Ackley, M. A.; Cass, C. E.; Young, J. D.; Baldwin, S. A. Nucleoside Transporters: From Scavengers to Novel Therapeutic Targets. *Trends Pharmacol. Sci.* **2006**, *27* (8), 416–425.

(55) Polonikov, A.; Sirotina, S.; Ponomarenko, I.; Shvetsov, Y.; Bykanova, M.; Bocharova, A.; Vagaytseva, K.; Stepanov, V.; Solodilova, M. AB074. Genetic Variation in CYP2U1, CYP4A11 and CYP4F2 Involved in the Biosynthesis of Hydroxyeicosatetraenoic Acids and Susceptibility to Hypertension and Atherosclerosis of Various Locations. *Ann. Transl. Med.* **2017**, *5* (S2), AB074–AB074.

(56) Hewitt, N. J.; Lechón, M. J. G.; Houston, J. B.; Hallifax, D.; Brown, H. S.; Maurel, P.; Kenna, J. G.; Gustavsson, L.; Lohmann, C.; Skonberg, C.; et al. Primary Hepatocytes: Current Understanding of the Regulation of Metabolic Enzymes and Transporter Proteins, and Pharmaceutical Practice for the Use of Hepatocytes in Metabolism, Enzyme Induction, Transporter, Clearance, and Hepatotoxicity Studies. *Drug Metab. Rev.* **2007**, *39*, 159–234.

(57) Prasad, B.; Bhatt, D. K.; Johnson, K.; Chapa, R.; Chu, X.; Salphati, L.; Xiao, G.; Lee, C.; Hop, C. E. C. A.; Mathias, A.; et al. Abundance of Phase 1 and 2 Drug-Metabolizing Enzymes in Alcoholic and Hepatitis C Cirrhotic Livers: A Quantitative Targeted Proteomics Study. *Drug Metab. Dispos.* **2018**, *46* (7), 943–952.

(58) Wolbold, R.; Klein, K.; Burk, O.; Nüssler, A. K.; Neuhaus, P.; Eichelbaum, M.; Schwab, M.; Zanger, U. M. Sex Is a Major Determinant of CYP3A4 Expression in Human Liver. *Hepatology* **2003**, *38*, 978–988.

(59) Galetin, A.; Brown, C.; Hallifax, D.; Ito, K.; Houston, J. B. Utility of Recombinant Enzyme Kinetics in Prediction of Human

Clearance: Impact of Variability, CYP3A5, and CYP2C19 on CYP3A4 Probe Substrates. *Drug Metab. Dispos.* **2004**, *32* (12), 1411–1420.

(60) King, B. P.; Leathart, J. B. S.; Mutch, E.; Williams, F. M.; Daly, A. K. CYP3A5 Phenotype-Genotype Correlations in a British Population. *Br. J. Clin. Pharmacol.* **2003**, *55* (6), 625–629.

(61) Rostami-Hodjegan, A.; Kroemer, H. K.; Tucker, G. T. In-Vivo Indices of Enzyme Activity: The Effect of Renal Impairment on the Assessment of CYP2D6 Activity. *Pharmacogenetics* **1999**, *9* (3), 277–286.

(62) Johnson, T. N.; Tucker, G. T.; Tanner, M. S.; Rostami-Hodjegan, A. Changes in Liver Volume from Birth to Adulthood: A Meta-Analysis. *Liver Transplant.* **2005**, *11* (11), 1481–1493.

(63) Barter, Z. E.; Chowdry, J. E.; Harlow, J. R.; Snawder, J. E.; Lipscomb, J. C.; Rostami-Hodjegan, A. Covariation of Human Microsomal Protein per Gram of Liver with Age: Absence of Influence of Operator and Sample Storage May Justify Interlaboratory Data Pooling. *Drug Metab. Dispos.* **2008**, *36* (12), 2405–2409.

(64) Polasek, T. M.; Patel, F.; Jensen, B. P.; Sorich, M. J.; Wiese, M. D.; Doogue, M. P. Predicted Metabolic Drug Clearance with Increasing Adult Age. *Br. J. Clin. Pharmacol.* **2013**, *75* (4), 1019–1028.

(65) Westlind-Johnsson, A.; Malmebo, S.; Johansson, A.; Otter, C.; Andersson, T. B.; Johansson, L.; Edwards, R. J.; Boobis, A. R.; Ingelman-Sundberg, M. Comparative Analysis of CYP3A Expression in Human Liver Suggests Only a Minor Role for CYP3A5 in Drug Metabolism. *Drug Metab. Dispos.* **2003**, *31* (6), 755–761.

(66) Zanger, U. M.; Fischer, J.; Raimundo, S.; Stüven, T.; Evert, B. O.; Schwab, M.; Eichelbaum, M. Comprehensive Analysis of the Genetic Factors Determining Expression and Function of Hepatic CYP2D6. *Pharmacogenetics* **2001**, *11*, 573–585.

(67) EMA. Reflection Paper on Investigation of Pharmacokinetics and Pharmacodynamics in the Obese Population. 2018, pp 1–11.

(68) Morgan, E. T. Impact of Infectious and Inflammatory Disease on Cytochrome P450-Mediated Drug Metabolism and Pharmacokinetics. *Clin. Pharmacol. Ther.* **2009**, *85* (4), 434–438.

(69) Margaillan, G.; Rouleau, M.; Klein, K.; Fallon, J. K.; Caron, P.; Villeneuve, L.; Smith, P. C.; Zanger, U. M.; Guillemette, C. Multiplexed Targeted Quantitative Proteomics Predicts Hepatic Glucuronidation Potential. *Drug Metab. Dispos.* **2015**, *43* (9), 1331–1335.

(70) Wortham, M.; Czerwinski, M.; He, L.; Parkinson, A.; Wan, Y. J. Y. Expression of Constitutive Androstane Receptor, Hepatic Nuclear Factor 4 $\alpha$ , and P450 Oxidoreductase Genes Determines Interindividual Variability in Basal Expression and Activity of a Broad Scope of Xenobiotic Metabolism Genes in the Human Liver. *Drug Metab. Dispos.* **2007**, *35* (9), 1700–1710.

(71) Izukawa, T.; Nakajima, M.; Fujiwara, R.; Yamanaka, H.; Fukami, T.; Takamiya, M.; Aoki, Y.; Ikushiro, S.; Sakaki, T.; Yokoi, T. Quantitative Analysis of UGT1A and UGT2B Expression Levels in Human Livers. *Drug Metab. Dispos.* **2009**, *37* (8), 1759–1768.